

JUL 8 1986

**NASA
Technical
Paper
2535**

C.2

April 1986

Low-Speed Stability and
Control Characteristics of
a Transport Model With
Aft-Fuselage-Mounted
Advanced Turboprops

Zachary T. Applin
and Paul L. Coe, Jr.

PROPERTY OF U.S. AIR FORCE
ADD TECHNICAL LIBRARY

**TECHNICAL REPORTS
FILE COPY**

NASA

**NASA
Technical
Paper
2535**

1986

Low-Speed Stability and
Control Characteristics of
a Transport Model With
Aft-Fuselage-Mounted
Advanced Turboprops

Zachary T. Applin
and Paul L. Coe, Jr.

*Langley Research Center
Hampton, Virginia*



National Aeronautics
and Space Administration

Scientific and Technical
Information Branch

Contents

Summary	1
Introduction	1
Symbols	1
Model	3
Tests and Corrections	3
Presentation of Results	3
Discussion of Results	4
Aerodynamic Characteristics of Isolated Propeller and Nacelle	4
Aerodynamic Characteristics of Advanced Turboprop Transport Model	4
Effect of thrust on longitudinal aerodynamic performance	4
Horizontal tail aerodynamic characteristics	5
Effect of thrust in ground effect	5
Effect of thrust on lateral-directional aerodynamic characteristics	5
Rudder aerodynamic characteristics	5
Engine-out characteristics	6
Summary of Results	6
Appendix -- Data for Longitudinal Stability Axis and Lateral Body Axis Systems	7
Tables	24
Figures	27
References	63

Summary

A limited experimental investigation was conducted in the Langley 4- by 7-Meter Tunnel to explore the effects of aft-fuselage-mounted advanced turboprop installations on the low-speed stability and control characteristics of a representative transport aircraft in a landing configuration.

In general, the experimental results indicate that the longitudinal and lateral-directional stability characteristics for the aft-fuselage-mounted single-rotation tractor and counter-rotation pusher propeller configurations tested during this investigation are acceptable aerodynamically. For the single-rotation tractor configuration, the propeller-induced aerodynamics are significantly influenced by the interaction of the propeller slipstream with the pylon and nacelle. This resulted in a nose-up or destabilizing pitching moment. The stability characteristics for the counter-rotation pusher configuration are strongly influenced by propeller normal forces. This configuration provided stabilizing pitching-moment characteristics and, above stall, a substantial increase in lift.

The longitudinal and directional control effectiveness, engine-out characteristics, and ground effects are also presented. In addition, a tabulated presentation of all aerodynamic data presented in this report is included as an appendix.

Introduction

Several studies have identified potentially significant fuel savings for advanced turboprop-powered transport aircraft (for example, refs. 1 and 2). The results of these studies indicate that both wing-mounted and aft-fuselage-mounted advanced turboprop configurations appear feasible and that configuration selection will depend on further information regarding acoustic treatment requirements, structural weight, and engine/airframe installation aerodynamics. Although decades of experience exist with propeller-driven aircraft, this experience has been for configurations having significantly lower power loadings than those presently considered. A major uncertainty associated with the aerodynamic characteristics of advanced turboprop aircraft configurations is the lack of information regarding the effect of the highly loaded turboprop installation on aircraft stability and control during the takeoff, climb, and landing phases of flight. These technical uncertainties are most pronounced for aft-fuselage-mounted turboprop configurations. This report addresses these technical uncertainties pertaining to the landing phase of the flight envelope.

The investigation discussed herein is part of a broad NASA research program to obtain fundamental aerodynamic information regarding advanced turboprop installation effects (ref. 3). This investigation was conducted with a representative advanced transport model modified to incorporate several arrangements of aft-fuselage-mounted single-rotation or counter-rotation propellers. This test examined an aft-fuselage-mounted single-rotation tractor configuration and an aft-fuselage-mounted counter-rotation pusher configuration with the aircraft model in a part-span-flap landing condition. The report describes test results in terms of aircraft stability and control as well as longitudinal and lateral-directional control surface effectiveness. Ground effects and engine-out characteristics are also presented. The tests were conducted in the Langley 4- by 7-Meter Tunnel for Reynolds numbers (based on wing mean geometric chord) of 0.51×10^6 and 0.93×10^6 .

Symbols

The longitudinal forces and moments presented in this report are referenced to the stability axis system, and the lateral-directional forces and moments are referenced to the body axis system. The moment data are referred to a moment center on the model centerline located at the longitudinal location of the wing quarter-chord point. This quarter-chord location is calculated for the mean geometric chord of the trapezoidal wing planform (without trailing-edge extension) that extends from the model centerline to the wing tip. The aerodynamic coefficient data are based on the trapezoidal wing planform, which has a reference area of 11.21 ft², a reference span of 10.59 ft, and a reference mean geometric chord of 13.44 in.

All measurements and calculations were made in U.S. Customary Units. The capitalized expression in parentheses next to the symbol is the computer printout equivalent of that symbol that is used in the tabulation of the aerodynamic data presented in the appendix.

b		wing span, ft
C_D	(CD)	drag coefficient, Drag/ qS
C_L	(CL)	lift coefficient, Lift/ qS
C_l	(CRM)	rolling-moment coefficient, Rolling moment/ qSb
$C_{l\beta}$		effective dihedral parameter based on increment of C_l between $\beta = -5^\circ$ and 5° , $\partial C_l / \partial \beta$, per degree

C_m	(CPM)	pitching-moment coefficient, Pitching moment/ $qS\bar{c}$	L/D	(L/D)	lift-drag ratio
			M	(MACH)	free-stream Mach number
C_N		normal-force coefficient (model reference system), Normal force/ qS	n		propeller rotational speed, rps
C'_N		normal-force coefficient (propeller reference system), Normal force/ qS_D	q	(Q)	free-stream dynamic pressure, lb/ft ²
C_n	(CYM)	yawing-moment coefficient (model reference system), Yawing moment/ qSb	S		wing reference area, ft ²
			S_D		propeller disk area, ft ²
C'_n		yawing-moment coefficient (propeller reference system), Yawing moment/ $qS_D d$	T_c		propeller thrust coefficient (model reference system), Propeller thrust/ qS
$C_{n\beta}$		directional stability parameter based on increment of C_n between $\beta = -5^\circ$ and 5° , $\partial C_n / \partial \beta$, per degree	T'_c		propeller thrust coefficient (propeller reference system), Propeller thrust/ qS_D
			$(t/c)_{\max}$		maximum airfoil thickness-chord ratio
C_T		propeller thrust coefficient (propeller reference system), Propeller thrust/ $\rho n^2 d^4$	V		free-stream velocity, ft/sec
C_Y	(CSF)	side-force coefficient (model reference system), Side force/ qS	y		lateral dimension, ft
			α	(ALPHA)	angle of attack of model reference centerline, positive nose up, deg
C'_Y		side-force coefficient (propeller reference system), Side force/ qS_D	β	(BETA)	angle of sideslip of model reference centerline, positive nose left, deg
$C_{Y\beta}$		side-force derivative based on increment of C_Y between $\beta = -5^\circ$ and 5° , $\partial C_Y / \partial \beta$, per degree	Δ		incremental value
			δ_r		rudder deflection angle, positive for trailing edge left, deg
c		reference mean geometric chord, in.	η		nondimensional wing semispan location
d		propeller diameter, ft	ρ		free-stream density, slugs/ft ³
h/b	(H/B)	height-span ratio of model moment reference center above floor, ft	Model components (fig. 9):		
			B		body
			G		landing gear
i_t		incidence of horizontal tail, positive for leading edge up, deg	HT		horizontal tail
			N		nacelle
J	(J)	propeller advance ratio, V/nd	P		pylon
			VT		vertical tail

W	wing
Abbreviations (fig. 7):	
CR	counter rotation
SR	single rotation

Model

Sketches of the model indicating the single-rotation tractor and counter-rotation pusher propeller configurations examined in this wind-tunnel test are shown in figure 1, and pertinent model geometric characteristics are summarized in table I. This model was obtained by modifying an existing Langley model from the NASA Energy Efficient Transport (EET) program. (See ref. 4 for a description of the original unmodified model.) The modifications consisted of increasing the fuselage length, removing the wing-mounted turbofan nacelles, and adding hardware options for various aft-fuselage-mounted pylons and nacelles. A detailed sketch of the aft end of this model indicating the geometric characteristics of both propeller configurations is presented in figure 2. The model high-lift system, which is the same as that described in references 4 and 5, consisted of a leading-edge slat deflected 50° and a two-segment trailing-edge flap system, with vane and flap each deflected 30° as shown in figure 3. Detailed coordinates of the wing and flap component surfaces are given in references 6 and 7. The landing gear arrangement was the same configuration used in references 4 and 5.

The single-rotation propeller tested was a model of the SR-2 eight-blade design and was 16.9 in. in diameter. The counter-rotation propeller also used the SR-2 eight-blade design, but with two four-blade propellers (referred to as "four-by-four blade propellers") turning in opposite directions, and it was 16.1 in. in diameter. Photographs of the single-rotation and counter-rotation propeller systems are presented in figure 4. Photographs of the model mounted for tests in the Langley 4- by 7-Meter Tunnel are shown in figure 5. Geometric characteristics of the SR-2 blades as well as of the pylon and nacelles are described in reference 8. Both the single-rotation and counter-rotation propeller systems were powered by a 29-hp (at 10 000 rpm) electric motor that provided maximum power loadings of 14.6 and 16.1 hp/ft², respectively. These power loadings are substantially lower than those currently considered for full-scale advanced turboprop applications. However, because the wind-tunnel velocity is a variable, properly matching the propeller characteristics in coefficient form enables the present tests to simulate the aerodynamics of higher power loading, advanced

turboprop concepts, as discussed in the appendix of reference 9.

Tests and Corrections

The tests were conducted in the Langley 4- by 7-Meter Tunnel, which has a test section 14.50 ft high by 21.75 ft wide by 50.0 ft long (ref. 10). The wind-tunnel tests were conducted at free-stream dynamic pressures of 6.0 and 20.0 lb/ft² with corresponding Reynolds numbers of 0.51×10^6 and 0.93×10^6 , based on the reference mean geometric chord of 13.44 in., and corresponding Mach numbers (M) of 0.06 and 0.12. The model was tested through an angle-of-attack range from -5° to 20° and an angle-of-sideslip range from -5° to 10° . Tests were conducted with the model positioned near the tunnel centerline to simulate free-stream conditions. Ground effect conditions were simulated by lowering the model toward the tunnel floor. According to reference 11, this method of ground effect simulation is appropriate for the conditions present during this investigation.

The aerodynamic forces and moments were measured with a six-component strain-gauge balance mounted inside the fuselage such that the model and balance moment centers were coincident along the model centerline. The balance characteristics are summarized in table II. The angle of attack was set by the pitch drive of the model support system and was measured by an electronic inclinometer mounted inside the forward portion of the fuselage. The sideslip angle was set by the yaw drive of the model support system and was measured by an electronic counter mounted to the yaw-drive gearing system.

Wind-tunnel jet-boundary corrections were determined according to reference 12 and were applied to the force and moment data. Wing, body, and wake solid-blockage corrections were also applied to the data and were determined according to reference 13. No corrections were made to the data because of tunnel flow angularity or support system interference.

Presentation of Results

The results and discussion are presented according to the following outline:

	Figure
Isolated propeller characteristics	6, 7
Longitudinal aerodynamic characteristics	8 to 12
Lateral-directional aerodynamic characteristics	13 to 18

Listed on the appropriate figures are the run numbers corresponding to the data plotted. The tabulated data for the longitudinal stability axis and

lateral body axis for all the runs presented in this report are given in the appendix.

Discussion of Results

The present investigation was conducted to obtain fundamental aerodynamic information regarding advanced turboprop installation effects. In order to understand the effect of the turboprop installation on the aircraft configuration, limited results that define the aerodynamic characteristics of the isolated propeller and nacelle are provided as background information.

Aerodynamic Characteristics of Isolated Propeller and Nacelle

The isolated propeller thrust coefficient C_T plotted against advance ratio J is shown in figure 6(a) for the single-rotation and counter-rotation propeller systems. All the aircraft model tests were conducted with a nominal propeller blade angle of 40° at the 75-percent propeller radius station. At the operating conditions used for these tests, this blade angle provided representative propeller thrust coefficients (ref. 9). Accordingly, the discussion of the aerodynamic characteristics of the isolated propeller and nacelle will be limited to this condition. The counter-rotation propeller achieves a higher thrust coefficient at a given advance ratio with the same number of blades as the single-rotation propeller. This increase in thrust is mainly attributed to the swirl recovery afforded by the aft propeller disk of the counter-rotation configuration. Propeller thrust coefficient has also been converted to aircraft model thrust coefficient T_c and is presented as a function of J in figure 6(b).

In addition to thrust effects, the propeller and nacelle configurations produce a normal force, yawing moment, and side force at angle of attack. These results are presented in propeller coefficient form in figure 7(a) and are also presented in aircraft model coefficient form in figure 7(b). As discussed in reference 9, the propeller side force and yawing moment produced at angle of attack result from the fact that at positive nacelle angle of attack, the downgoing blade experiences a higher local blade angle of attack than the upgoing blade. This higher blade angle of attack produces a higher thrust for the downgoing blade (relative to the upgoing blade) and, consequently, a higher pressure rise across the propeller disk on the downgoing side, again relative to the upgoing side. This pressure rise difference leads to a slipstream crossflow that acts on the nacelle. It is this crossflow acting on the nacelle that produces the side force and yawing moment shown in figure 7 for the single-rotation system.

The side force is significantly reduced for the counter-rotation system (composed of two propellers turning in opposite directions) compared with the single-rotation system. The propeller normal force results from flow turning as it passes through the propeller disk at angle of attack. The substantially higher normal force produced by the counter-rotating propellers indicates that the counter-rotation system is more effective in turning the flow.

Aerodynamic Characteristics of Advanced Turboprop Transport Model

Effect of thrust on longitudinal aerodynamic performance. The static longitudinal aerodynamic characteristics for the transport model configuration with the single-rotation tractor and the counter-rotation pusher propellers are presented in figure 8. The values of aircraft thrust coefficient were obtained from figure 6(b), based on the propeller advance ratio and blade angle.

Increasing thrust has a minimal effect on C_L for both propeller configurations over most of the angle-of-attack range. At angles of attack above stall, the propeller normal-force contribution to vehicle lift is greater for the counter-rotation configuration than for the single-rotation configuration. The differences between the power-off and power-on drag polars show a shift roughly equivalent to propeller thrust ($T_c \times 2$). (The scatter in the values of C_D for the single-rotation tractor configuration ($J = 1.01$) case results from the difficulties in holding both propeller and tunnel operating conditions constant and in measuring the low balance drag load for this test condition.)

Thrust effects on pitching moment are different for the two propeller configurations. For the single-rotation tractor propeller, the principal effect of thrust is a nose-up, or positive, increment in C_m . As shown in figure 2, the propeller thrust line is above the model moment center, so the moment resulting from thrust increase was expected to be nose down. The reason for this nose-up increment is partially explained by the unpowered aerodynamic data presented in figure 9. This figure shows the effect on longitudinal aerodynamic characteristics due to the addition of the horizontal tail, pylon, and nacelles to the unpowered aircraft configuration. The addition of the pylon and nacelles results in a positive increment in C_m and an increase in static longitudinal stability. For the single-rotation tractor configuration, the pylon and nacelles are immersed in the high-velocity propeller slipstream that accentuates their effect essentially throughout the angle-of-attack range. The primary reason for the positive increment in pitching moment, however, is probably

related to the direction of propeller rotation. During these tests, the single-rotation propellers rotated downward inboard. This would result in an effective downwash (related to the swirl component of velocity in the propeller slipstream) acting on the pylon surfaces; this downwash results in a positive increment in pitching moment.

By contrast, the pitching-moment characteristics for the configuration with the counter-rotation pusher installation (fig. 8(b)) show a marked increase in longitudinal stability with increasing thrust and angle of attack. As angle of attack is increased, the large normal force produced by the counter-rotation propeller system provides a strong stabilizing force that continues beyond the loss in horizontal tail effectiveness. The thrust effects noted for both turboprop configurations would not adversely affect the aerodynamic feasibility of these arrangements.

Horizontal tail aerodynamic characteristics. The effect of horizontal tail deflection on the longitudinal aerodynamic characteristics is presented in figure 10. The effect of thrust on horizontal tail control effectiveness is presented in figure 11. As shown, the horizontal tail effectiveness was not significantly influenced by increasing thrust for either propeller configuration.

Effect of thrust in ground effect. Ground effect tests were conducted and the results are presented in figure 12 for the model at an angle of attack of 8° . For the power-off condition, the data show a reduction in drag and an increase in nose-down pitching moment as the height above the ground h/b is reduced. Similar trends were obtained previously for the turbofan-configured model, and the results are discussed in reference 5. With power on, both propeller configurations had trends similar to the power-off condition.

Effect of thrust on lateral-directional aerodynamic characteristics. The effect of sideslip on the lateral-directional aerodynamic stability characteristics for the power-off case and for both propeller configurations is presented in figure 13. The static lateral-directional stability derivatives derived from these data are presented in figure 14 for each propeller configuration compared with the power-off case. The power-off lateral-directional stability characteristics obtained were very similar to those of the unmodified turbofan model. (See ref. 5.)

For the single-rotation tractor configuration, increments in the effective dihedral parameter C_{l_β} between the power-off and two power-on conditions

were the result of the propeller side force. (See fig. 7.) As the model was sideslipped, each propeller was at a sideslip incidence angle that produced a propeller side force which resulted in a model normal force. Since the direction of propeller rotation on either side of the model was opposite, the normal force produced by each propeller was of opposite sign. This generated a net negative aircraft-model rolling moment that increased with thrust at low angles of attack (fig. 14). There was also a departure from the power-off curve above the stall angle of attack. There was a minimal influence of thrust on the directional stability parameter C_{n_β} and the side-force parameter C_{Y_β} for angles of attack below stall.

For the counter-rotation pusher configuration, increasing thrust had a minimal effect on C_{l_β} . This was due to the fact that the side force produced by the counter-rotation propeller at angle of incidence was substantially lower than that by the single-rotation propeller. However, an increase in C_{n_β} resulted from adding thrust to the counter-rotation pusher configuration. As was the case with longitudinal stability, the increase in C_{n_β} is directly related to the propeller normal force produced by the counter-rotation system at angle of attack. In the directional sense, sideslip would represent an incidence angle in the lateral plane and, thus, the propeller would produce both a negative side force (corresponding to the previously discussed propeller normal force) and a restoring moment. The slight negative increment C_{Y_β} is probably a component of this propeller normal force.

Rudder aerodynamic characteristics. The effect of rudder deflection on the lateral-directional aerodynamic characteristics is presented in figure 15. The effect of thrust on C_n plotted against δ_r (a measure of rudder effectiveness) is shown in figure 16. For the single-rotation tractor configuration, the rudder effectiveness is increased with the addition of thrust. The slipstream generated by the tractor propeller increased the dynamic pressure on the rudder, and the slipstream deflection caused by the rudder increased its effectiveness. An opposite effect was noted for the counter-rotation pusher configuration. As shown in figure 16(b), for this configuration the rudder effectiveness was reduced with increasing thrust. It is possible that the sidewash generated by rudder deflection produced an effective flow angularity at the propeller plane. This effective propeller yaw angle would produce propeller forces causing an aircraft yawing moment opposing that produced by rudder deflection. In comparison with the tractor configuration,

the rudder has no opportunity to deflect the propeller slipstream of the pusher configuration.

Engine-out characteristics. The effect of right engine out (propeller allowed to windmill) on the lateral-directional aerodynamic characteristics is presented in figure 17 for both propeller configurations. In each case a rudder deflection of 30° was applied to provide a restoring moment to the asymmetric condition generated by the right propeller windmilling. In all cases, except for the counter-rotation pusher configuration of $J = 0.92$ (fig. 17(d)), this rudder deflection was sufficient to overcome the asymmetric engine-out yawing moment.

Data for the engine-out yawing moment of the single-rotation tractor configuration are presented in figure 18. Also presented is the theoretical variation of C_n with T_c based on the simple relationship

$$C_n = T_c \frac{y}{b}$$

Inasmuch as the engine-out tests were conducted with the "inoperative" propeller allowed to windmill, the indicated theoretical result should underpredict the actual moment by an amount corresponding to the moment increment associated with windmilling drag. Thus, the engine-out yawing moment was approximately equal to the moment produced by lateral thrust and drag offsets.

Summary of Results

The results of a limited experimental investigation to explore the effects of aft-fuselage-mounted advanced turboprop installations on the low-speed stability and control characteristics of a representative transport aircraft model in a landing configuration are summarized as follows:

1. The overall longitudinal and lateral-directional stability characteristics of the configuration were not adversely affected by either the aft-fuselage-mounted single-rotation tractor propeller or counter-rotation pusher propeller as compared with the baseline unpowered configuration.
2. The interaction of the propeller slipstream with the pylon and nacelle had a significant effect on longitudinal stability for the single-rotation tractor configuration (with propellers rotating downward inboard). This resulted in a nose-up or destabilizing pitching moment.
3. The propeller normal forces had a significant effect on longitudinal stability for the counter-rotation pusher configuration. This configuration provided stabilizing pitching-moment characteristics, and above stall it provided a substantial increase in lift.
4. The effects of thrust on horizontal tail effectiveness were minimal for both propeller configurations.
5. Both propeller configurations had ground effect trends similar to those of the unpowered condition.
6. The single-rotation tractor propeller increased the rudder effectiveness by increasing the dynamic pressure on the rudder. The counter-rotation pusher propeller decreased the rudder effectiveness by producing a yawing moment opposing that produced by rudder deflection.
7. The engine-out asymmetric yawing-moment characteristics were approximately equal to moments produced by lateral thrust and drag offset.

NASA Langley Research Center
Hampton, VA 23665-5225
December 11, 1985

RUN NUMBER 209 LONGITUDINAL STABILITY AXIS AND LATERAL BODY AXIS DATA TEST NUMBER 284

Table with 13 columns: MACH, Q, PSF, BETA, DEG, ALPHA, DEG, J, CL, CD, CPM, CRM, CYM, CSF, L/D, 4/B. Rows show data for MACH 0.090 to 11.98 and Q, PSF 11.98 to 12.09.

RUN NUMBER 211 LONGITUDINAL STABILITY AXIS AND LATERAL BODY AXIS DATA TEST NUMBER 284

Table with 13 columns: MACH, Q, PSF, BETA, DEG, ALPHA, DEG, J, CL, CD, CPM, CRM, CYM, CSF, L/D, 4/B. Rows show data for MACH 0.065 to 0.64 and Q, PSF 6.33 to 5.99.

RUN NUMBER 212 LONGITUDINAL STABILITY AXIS AND LATERAL BODY AXIS DATA TEST NUMBER 284

Table with 13 columns: MACH, Q, PSF, BETA, DEG, ALPHA, DEG, J, CL, CD, CPM, CRM, CYM, CSF, L/D, 4/B. Rows show data for MACH 0.090 to 11.87 and Q, PSF 12.21 to 11.87.

RUN NUMBER 217 LONGITUDINAL STABILITY AXIS AND LATERAL BODY AXIS DATA TEST NUMBER 284

Table with 13 columns: MACH, Q, PSF, BETA, DEG, ALPHA, DEG, J, CL, CD, CPM, CYM, CSF, L/D, 4/B. Rows show data for MACH 0.065 to 0.63 and Q, PSF 6.33 to 5.99.

RUN NUMBER 274				LONGITUDINAL STABILITY AXIS AND LATERAL BODY AXIS DATA								TEST NUMBER 284	
MACH	Q,PSF	BETA,DEG	ALPHA,DEG	J	CL	CD	CPM	CRM	CYM	CSF	L/D	H/B	
.091	12.32	.00	-4.98	****	-.2318	.2299	1.3728	-.0017	-.0017	.0065	-1.01	.587	
.091	12.32	.00	-3.08	****	.1468	.2781	1.1337	-.0068	.0000	.0012	.53	.591	
.090	12.09	.00	-.92	****	.5423	.2514	.9710	-.0053	-.0023	.0071	2.16	.594	
.090	11.98	.00	.15	****	.6806	.2406	.9134	.0061	-.0037	.0106	2.83	.596	
.090	11.98	.00	1.15	****	.8422	.2545	.8408	-.0046	-.0024	.0049	3.31	.598	
.090	11.98	.00	2.07	****	1.0059	.2661	.7779	-.0026	-.0025	.0074	3.78	.600	
.089	11.87	.00	3.25	****	1.1749	.2579	.7329	-.0012	-.0013	.0083	4.36	.602	
.090	11.98	.00	4.14	****	1.2278	.2677	.6716	-.0016	-.0020	.0090	4.59	.604	
.089	11.87	.00	5.91	****	1.4429	.2627	.5743	.0016	-.0019	.0070	5.49	.608	
.089	11.75	.00	8.02	****	1.6365	.2822	.4532	-.0009	-.0017	.0068	5.80	.612	
.089	11.87	.00	10.31	****	1.9003	.2872	.2989	.0015	-.0018	.0064	6.62	.617	
.089	11.76	.00	12.02	****	2.0553	.3260	.2031	.0013	-.0015	.0026	6.30	.620	
.089	11.87	.00	14.19	****	2.2224	.3654	.0872	-.0007	-.0051	.0057	6.08	.625	
.089	11.64	.00	16.02	****	2.2684	.4093	.0354	-.0087	-.0096	.0097	5.54	.629	
.089	11.64	.00	17.95	****	2.2923	.4812	-.0445	-.0070	-.0094	-.0028	4.76	.634	
.089	11.64	.00	20.08	****	2.2646	.5486	-.0296	.0079	-.0018	-.0021	4.13	.638	

RUN NUMBER 275				LONGITUDINAL STABILITY AXIS AND LATERAL BODY AXIS DATA								TEST NUMBER 284	
MACH	Q,PSF	BETA,DEG	ALPHA,DEG	J	CL	CD	CPM	CRM	CYM	CSF	L/D	H/B	
.091	12.21	.00	-5.06	****	.0439	.1196	.3137	-.0030	-.0018	.0146	.37	.587	
.091	12.21	.00	-2.97	****	.4097	.1674	.0366	-.0062	-.0010	.0102	2.45	.591	
.090	12.09	.00	-1.00	****	.8472	.1760	-.1667	-.0001	-.0039	.0180	4.81	.594	
.090	12.09	.00	.11	****	1.0246	.1773	-.2627	-.0007	-.0033	.0154	5.78	.596	
.090	11.98	.00	1.11	****	1.1726	.2061	-.3378	-.0011	-.0046	.0190	5.69	.598	
.090	11.98	.00	2.22	****	1.3134	.2064	-.4115	-.0001	-.0036	.0161	6.36	.600	
.089	11.87	.00	3.11	****	1.4298	.2255	-.4597	-.0041	-.0042	.0187	6.34	.602	
.089	11.75	.00	4.21	****	1.5733	.2290	-.5440	.0004	-.0025	.0125	6.87	.604	
.089	11.87	.00	6.21	****	1.7434	.2383	-.6557	.0012	-.0021	.0134	7.32	.608	
.089	11.75	.00	8.05	****	2.0040	.2652	-.7974	.0020	-.0015	.0166	7.56	.612	
.089	11.75	.00	10.09	****	2.1804	.3093	-.9066	-.0003	-.0012	.0105	7.05	.616	
.089	11.75	.00	12.36	****	2.3996	.3244	-1.0492	-.0028	-.0029	.0092	7.40	.621	
.089	11.64	.00	14.15	****	2.5593	.3728	-1.1578	.0013	-.0009	-.0028	6.86	.625	
.089	11.64	.00	16.29	****	2.5700	.4221	-1.1901	-.0087	-.0093	.0078	6.09	.630	
.089	11.64	.00	17.95	****	2.5565	.5009	-1.1932	-.0043	-.0084	.0086	5.10	.634	
.088	11.53	.00	20.08	****	2.5178	.6037	-1.1556	.0074	.0001	-.0026	4.17	.638	

RUN NUMBER 276				LONGITUDINAL STABILITY AXIS AND LATERAL BODY AXIS DATA								TEST NUMBER 284	
MACH	Q,PSF	BETA,DEG	ALPHA,DEG	J	CL	CD	CPM	CRM	CYM	CSF	L/D	H/B	
.091	12.32	.00	-5.06	****	.7114	.1817	-.0982	-.0011	-.0021	.0085	1.16	.587	
.091	12.32	.00	-3.12	****	.5725	.2260	-.3738	-.0049	-.0024	.0085	2.53	.590	
.090	12.09	.00	-1.15	****	.9126	.2272	-.5690	-.0018	-.0024	.0147	4.02	.594	
.089	11.87	.00	.08	****	1.1249	.2351	-.6838	-.0017	-.0035	.0129	4.78	.596	
.089	11.75	.00	1.08	****	1.3017	.2495	-.7555	.0003	-.0030	.0168	5.22	.598	
.089	11.76	.00	2.11	****	1.4232	.2485	-.8266	.0045	-.0019	.0143	5.73	.600	
.089	11.75	.00	3.11	****	1.5566	.2751	-.8951	.0022	-.0014	.0108	5.66	.602	
.089	11.75	.00	4.07	****	1.7014	.2826	-.9641	.0002	-.0007	.0139	6.02	.604	
.089	11.75	.00	6.13	****	1.8973	.3044	-1.0776	-.0001	-.0010	.0078	6.23	.608	
.089	11.64	.00	8.13	****	2.0706	.3045	-1.1773	.0031	.0001	.0170	6.80	.612	
.089	11.64	.00	10.05	****	2.2656	.3326	-1.2890	.0008	-.0016	.0112	6.81	.616	
.088	11.53	.00	11.95	****	2.4725	.3966	-1.4023	.0005	-.0009	.0101	6.23	.620	
.088	11.53	.00	14.04	****	2.5957	.4421	-1.4573	-.0007	-.0032	.0073	5.87	.625	
.088	11.53	.00	16.06	****	2.6045	.5213	-1.4091	-.0149	-.0110	.0052	5.00	.629	
.088	11.53	.00	17.95	****	2.5834	.6014	-1.4028	-.0046	-.0082	.0042	4.30	.633	
.087	11.30	.00	20.08	****	2.5670	.7086	-1.4134	.0091	.0031	-.0110	3.62	.638	

RUN NUMBER 277				LONGITUDINAL STABILITY AXIS AND LATERAL BODY AXIS DATA								TEST NUMBER 284	
MACH	Q,PSF	BETA,DEG	ALPHA,DEG	J	CL	CD	CPM	CRM	CYM	CSF	L/D	H/B	
.091	12.21	.00	-5.07	****	-.0211	.2459	.6352	-.0157	.0325	-.0854	-.09	.587	
.091	12.21	.00	-2.95	****	.3638	.2281	.4240	-.0113	.0309	-.0805	1.59	.598	
.091	12.21	.00	-.98	****	.7280	.2460	.2212	-.0133	.0287	-.0749	2.96	.591	
.091	12.21	.00	.06	****	.9104	.2502	.1185	-.0054	.0301	-.0779	3.64	.593	
.091	12.09	.00	1.10	****	1.0889	.2595	.0343	-.0137	.0276	-.0747	4.20	.595	
.090	11.98	.00	1.87	****	1.2058	.2826	-.0349	-.0093	.0292	-.0807	4.27	.597	
.090	11.98	.00	3.05	****	1.3525	.2727	-.0917	-.0096	.0299	-.0753	4.96	.599	
.090	11.87	.00	4.05	****	1.4659	.2744	-.1601	-.0116	.0286	-.0778	5.34	.601	
.091	12.09	.00	6.08	****	1.6776	.3012	-.2893	-.0092	.0292	-.0792	5.57	.605	
.091	12.21	.00	8.00	****	1.8928	.3177	-.4104	-.0088	.0315	-.0830	5.96	.609	
.091	12.09	.00	10.11	****	2.0996	.3274	-.5395	-.0076	.0305	-.0808	6.41	.613	
.091	12.21	.00	12.04	****	2.2825	.3650	-.6811	-.0066	.0314	-.0839	6.25	.618	
.090	11.98	.00	13.94	****	2.4253	.4028	-.7645	-.0114	.0296	-.0941	6.02	.622	
.091	12.09	.00	16.01	****	2.4812	.4597	-.8552	-.0175	.0250	-.0954	5.40	.626	
.090	11.87	.00	18.01	****	2.4862	.5507	-.8988	-.0114	.0224	-.0951	4.51	.631	
.090	11.98	.00	20.07	****	2.4522	.6103	-.8910	.0014	.0240	-.0817	4.02	.635	

RUN NUMBER 338		LONGITUDINAL STABILITY AXIS AND LATERAL BODY AXIS DATA										TEST NUMBER 284	
MACH	Q,PSF	BETA,DEG	ALPHA,DEG	J	CL	CD	CPM	CRM	CYM	CSF	L/D	H/B	
.065	6.33	.00	8.08	1.03	1.8332	-.2032	-.5908	.0063	-.0019	-.0015	-9.02	.088	
.066	6.44	.00	8.12	1.04	1.8650	-.1872	-.5428	.0048	-.0002	-.0002	-9.96	.131	
.065	6.33	.00	7.94	1.03	1.8883	-.1302	-.4386	.0030	.0006	-.0133	-14.50	.199	
.065	6.33	.00	7.97	1.03	1.8415	-.1257	-.3595	-.0013	-.0011	-.0167	-14.65	.268	
.064	6.10	.00	7.97	1.01	1.8157	-.1296	-.2127	.0042	-.0011	-.0130	-14.01	.404	
.064	6.10	.00	8.01	1.02	1.8353	-.1358	-.1933	.0052	-.0026	-.0080	-13.51	.542	
.064	5.99	.00	8.01	1.01	1.8350	-.1485	-.1724	.0087	-.0021	-.0038	-12.35	.623	

RUN NUMBER 339		LONGITUDINAL STABILITY AXIS AND LATERAL BODY AXIS DATA										TEST NUMBER 284	
MACH	Q,PSF	BETA,DEG	ALPHA,DEG	J	CL	CD	CPM	CRM	CYM	CSF	L/D	H/B	
.091	12.32	.00	8.01	1.40	1.8715	.0482	-.6552	.0034	-.0022	.0001	38.86	.088	
.092	12.43	.00	8.05	1.41	1.9565	.0731	-.6416	-.0008	-.0018	-.0062	26.78	.131	
.091	12.32	.00	8.01	1.40	1.9220	.0939	-.5149	-.0026	-.0008	-.0122	20.47	.199	
.091	12.21	.00	8.08	1.41	1.9085	.1030	-.4398	-.0032	-.0004	-.0149	13.53	.268	
.090	11.98	.00	8.16	1.41	1.8878	.1115	-.3523	.0012	-.0004	-.0107	16.93	.405	
.090	11.87	.00	8.12	1.40	1.8609	.1163	-.3160	.0087	.0000	-.0022	16.00	.542	
.090	12.09	.00	8.05	1.41	1.8841	.1300	-.3176	.0078	-.0013	.0025	14.49	.623	

RUN NUMBER 341		LONGITUDINAL STABILITY AXIS AND LATERAL BODY AXIS DATA										TEST NUMBER 244	
MACH	Q,PSF	BETA,DEG	ALPHA,DEG	J	CL	CD	CPM	CRM	CYM	CSF	L/D	H/B	
.064	5.99	.00	-5.03	1.01	-.1214	.0127	.8032	-.0150	.0258	.0159	-9.56	.587	
.064	5.99	.00	-2.97	1.01	.2832	.0112	.5930	-.0126	.0274	.0104	25.19	.591	
.064	5.99	.00	-1.00	1.01	.6461	.0234	.4240	-.0117	.0250	.0158	27.56	.594	
.064	5.99	.00	.00	1.00	.8580	.0310	.2952	-.0097	.0260	.0126	27.67	.596	
.064	5.99	.00	1.11	1.00	.9901	-.0091	.2195	-.0063	.0279	.0117	-109.32	.598	
.064	5.99	.00	2.07	1.00	1.1546	.0318	.1377	.0001	.0304	-.0051	36.28	.600	
.064	5.99	.00	2.92	1.00	1.2423	.0547	.0740	.0000	.0290	-.0019	22.72	.602	
.063	5.88	.00	4.13	.99	1.3874	.0471	.0027	-.0012	.0311	-.0014	29.44	.604	
.064	6.10	.00	6.02	1.01	1.5813	.0835	-.1349	-.0014	.0312	.0046	18.93	.608	
.065	6.22	.00	8.08	1.02	1.8024	.0661	-.2649	-.0024	.0323	-.0017	27.27	.512	
.064	6.10	.00	10.08	1.01	2.0551	.1384	-.4051	-.0032	.0319	-.0027	14.84	.516	
.065	6.22	.00	11.94	1.02	2.2199	.1645	-.5368	-.0019	.0343	-.0209	13.49	.520	
.064	6.10	.00	13.95	1.01	2.3670	.1977	-.6415	-.0096	.0288	-.0112	11.98	.625	
.064	6.10	.00	16.09	1.01	2.4210	.2193	-.7268	-.0066	.0269	-.0074	11.09	.629	
.064	6.10	.00	18.13	1.01	2.3844	.2782	-.8004	.0017	.0325	-.0180	8.57	.634	
.064	5.99	.00	19.96	1.00	2.4139	.4438	-.7995	.0024	.0304	.0050	5.44	.638	

RUN NUMBER 342		LONGITUDINAL STABILITY AXIS AND LATERAL BODY AXIS DATA										TEST NUMBER 284	
MACH	Q,PSF	BETA,DEG	ALPHA,DEG	J	CL	CD	CPM	CRM	CYM	CSF	L/D	H/B	
.090	12.09	.00	-4.99	1.43	-.0954	.1308	.7148	-.0066	.0072	.0063	-4.73	.587	
.090	11.87	.00	-3.12	1.40	.2255	.1381	.5384	.0005	.0071	.0052	1.65	.590	
.090	11.87	.00	-.97	1.40	.6405	.1258	.3045	.0045	.0054	.0143	5.09	.594	
.089	11.75	.00	-.08	1.40	.8391	.1455	.2385	-.0004	.0063	.0134	5.77	.596	
.089	11.75	.00	.96	1.40	1.0075	.1553	.1342	-.0038	.0066	.0157	6.49	.598	
.089	11.75	.00	2.03	1.39	1.1752	.1628	.0459	-.0015	.0073	.0097	7.22	.600	
.089	11.64	.00	2.92	1.41	1.3283	.1806	-.0243	.0026	.0090	.0083	7.35	.602	
.090	11.87	.00	4.17	1.42	1.4616	.1794	-.1128	.0029	.0088	.0006	8.15	.604	
.090	11.87	.00	6.09	1.42	1.6862	.1926	-.2351	-.0028	.0075	.0055	8.75	.608	
.089	11.75	.00	8.08	1.41	1.8877	.2203	-.3532	.0059	.0125	-.0002	8.57	.612	
.089	11.75	.00	12.09	1.41	2.2926	.2771	-.6036	-.0006	.0099	.0040	8.27	.621	
.089	11.76	.00	13.95	1.41	2.4370	.3398	-.7125	-.0037	.0074	.0019	7.17	.625	
.089	11.75	.00	16.20	1.41	2.4699	.3705	-.8147	-.0096	.0058	-.0022	6.67	.630	
.090	11.98	.00	17.98	1.43	2.4345	.4464	-.8003	-.0044	.0065	.0037	5.45	.634	
.090	11.87	.00	18.13	1.42	2.4545	.4451	-.8148	-.0035	.0056	.0009	5.51	.634	
.089	11.76	.00	20.15	1.40	2.4434	.5372	-.8735	.0096	.0132	-.0083	4.55	.638	

RUN NUMBER 344		LONGITUDINAL STABILITY AXIS AND LATERAL BODY AXIS DATA										TEST NUMBER 284	
MACH	Q,PSF	BETA,DEG	ALPHA,DEG	J	CL	CD	CPM	CRM	CYM	CSF	L/D	H/B	
.064	5.99	.00	-5.03	1.01	-.1345	-.0156	.8579	-.0042	-.0061	.0091	8.63	.597	
.064	5.99	.00	-3.09	1.01	.2170	.0390	.6217	.0002	-.0085	.0100	5.72	.590	
.063	5.88	.00	-.97	1.01	.6594	-.0036	.4005	.0012	-.0072	.1028	-182.87	.594	
.064	5.99	.00	.00	1.02	.7993	.0070	.3173	.0132	-.0078	.0909	114.40	.596	
.064	5.99	.00	1.03	1.02	.9625	.0137	.2403	.0091	-.0081	.1083	70.20	.598	
.063	5.88	.00	2.18	1.00	1.1334	.0076	.1765	.0059	-.0049	.1007	148.87	.600	
.063	5.88	.00	2.99	1.01	1.2326	.0530	.1346	.0022	-.0051	.1049	23.25	.602	
.063	5.88	.00	4.10	1.00	1.3946	.0320	.0268	.0054	-.0020	.0847	43.62	.604	
.062	5.76	.00	5.98	1.00	1.5780	.0412	-.1537	.0053	.0004	.0901	40.76	.608	
.063	5.88	.00	8.08	1.01	1.8440	.0627	-.2916	.0095	.0037	.0872	29.39	.612	
.062	5.76	.00	10.16	1.00	2.0688	.0885	-.4096	.0069	.0015	.0809	23.37	.616	
.062	5.76	.00	12.05	1.00	2.2664	.1420	-.5667	.0076	.0048	.0832	15.96	.620	
.062	5.76	.00	14.03	.99	2.3661	.1948	-.6325	-.0032	-.0028	.0921	12.15	.625	
.063	5.88	.00	16.05	1.01	2.4025	.2131	-.6977	-.0016	-.0055	.0893	11.27	.629	
.065	6.22	.00	18.02	1.03	2.3957	.3094	-.7254	.0083	-.0027	.0850	7.74	.634	
.065	6.22	.00	20.04	1.03	2.3537	.3854	-.6981	.0060	-.0023	.0844	6.11	.638	

LONGITUDINAL STABILITY AXIS AND LATERAL BODY AXIS DATA												TEST NUMBER 284	
MACH	Q, PSF	RETA, DEG	ALPHA, DEG	J	CL	CD	CPM	CRM	CYM	CSF	L/D	H/B	
.090	12.09	.00	-4.99	1.40	-.0920	.1296	.7344	.0026	-.0282	.1052	-1.71	.587	
.090	11.98	.00	-2.97	1.40	-.2508	.1346	.9290	.0067	-.0285	.1058	1.86	.591	
.090	11.98	.00	-1.00	1.39	.6540	.1362	.3339	.0136	-.0277	.1079	4.80	.594	
.090	11.98	.00	.14	1.40	.8554	.1400	.2231	.0138	-.0279	.1081	6.11	.596	
.090	11.87	.00	.99	1.40	1.0008	.1687	.1596	.0067	-.0283	.1072	5.93	.598	
.089	11.76	.00	1.96	1.39	1.1937	.1688	.0820	.0056	-.0269	.1043	7.07	.600	
.090	11.98	.00	3.06	1.40	1.3284	.1846	.0021	.0107	-.0251	.0942	7.20	.602	
.090	11.98	.00	4.06	1.41	1.4397	.1878	-.0662	.0070	-.0257	.1022	7.67	.604	
.090	11.87	.00	6.09	1.40	1.6519	.2090	-.2099	.0072	-.0249	.1073	7.90	.608	
.089	11.75	.00	8.12	1.39	1.8948	.2175	-.3455	.0093	-.0227	.0953	8.66	.612	
.090	11.87	.00	10.12	1.40	2.1163	.2588	-.4870	.0109	-.0209	.0898	8.18	.616	
.090	11.87	.00	12.20	1.40	2.2886	.2757	-.6122	.0077	-.0227	.0929	8.30	.621	
.090	11.87	.00	14.03	1.40	2.4341	.3190	-.7265	.0060	-.0231	.0885	7.63	.625	
.090	12.09	.00	15.90	1.41	2.4729	.3956	-.7866	-.0016	-.0277	.0918	6.25	.629	
.090	12.09	.00	18.25	1.41	2.4679	.4409	-.8096	.0030	-.0259	.0960	5.60	.634	
.090	11.98	.00	20.08	1.41	2.4732	.5269	-.7949	.0134	-.0193	.0917	4.69	.638	

LONGITUDINAL STABILITY AXIS AND LATERAL BODY AXIS DATA												TEST NUMBER 284	
MACH	Q, PSF	RETA, DEG	ALPHA, DEG	J	CL	CD	CPM	CRM	CYM	CSF	L/D	H/B	
.092	12.21	.03	-5.05	****	.0294	.2027	.6127	-.0076	.0023	.0038	.14	.585	
.092	12.21	.03	-2.96	****	.3477	.1785	.4171	.0004	-.0005	.0017	1.95	.589	
.091	12.09	.03	-1.03	****	.7555	.1768	.2677	.0120	.0012	.0002	4.27	.592	
.092	12.21	.03	.09	****	.9264	.1909	.2133	.0033	-.0001	.0043	4.85	.594	
.092	12.21	.03	1.08	****	1.0084	.1985	.0814	.0046	-.0004	.0043	5.08	.596	
.091	12.09	.03	2.19	****	1.2281	.1931	-.0269	-.0016	-.0007	.0112	6.36	.598	
.091	12.09	.03	3.15	****	1.3672	.2045	-.1014	.0045	.0014	.0042	6.68	.600	
.091	11.98	.03	4.08	****	1.4325	.2192	-.1462	.0050	-.0003	.0034	6.53	.602	
.092	12.21	.03	6.11	****	1.6536	.2332	-.3110	.0089	.0017	-.0004	7.09	.606	
.092	12.43	.03	8.17	****	1.8641	.2534	-.4226	.0031	.0022	.0051	7.36	.610	
.092	12.32	.03	9.99	****	2.0897	.2885	-.5302	.0051	-.0008	.0112	7.24	.614	
.092	12.32	.03	11.96	****	2.2902	.3044	-.6597	.0024	.0035	-.0072	7.49	.618	
.092	12.32	.03	14.04	****	2.4609	.3536	-.7953	.0093	.0004	.0092	6.96	.623	
.092	12.21	.03	15.92	****	2.4315	.4287	-.8397	-.0034	-.0070	.0227	5.67	.627	
.092	12.21	.03	18.11	****	2.4489	.4993	-.8977	-.0090	-.0073	.0265	4.90	.632	
.092	12.21	.03	20.21	****	2.4191	.5657	-.8536	-.0018	-.0060	.0329	4.28	.637	

LONGITUDINAL STABILITY AXIS AND LATERAL BODY AXIS DATA												TEST NUMBER 284	
MACH	Q, PSF	RETA, DEG	ALPHA, DEG	J	CL	CD	CPM	CRM	CYM	CSF	L/D	H/B	
.092	12.21	-5.00	-4.94	****	-.1025	.1687	.6201	-.0124	-.0170	.1454	-1.61	.587	
.091	11.98	-5.00	-2.88	****	.3095	.1751	.4071	-.0036	-.0173	.1413	1.77	.591	
.091	12.09	-5.00	-1.03	****	.6835	.1590	.2234	.0113	-.0209	.1415	4.30	.594	
.091	12.09	-5.00	.01	****	.9030	.1711	.1516	.0194	-.0188	.1393	5.28	.596	
.092	12.21	-5.00	1.05	****	.9947	.1737	.0586	.0155	-.0173	.1296	5.73	.598	
.091	12.09	-5.00	2.30	****	1.2095	.1814	-.0935	.0183	-.0193	.1321	6.67	.600	
.091	11.98	-5.00	3.08	****	1.3146	.1974	-.0264	.0215	-.0175	.1218	6.66	.602	
.091	12.09	-5.00	3.97	****	1.3952	.2099	-.1384	.0214	-.0173	.1246	6.68	.604	
.090	11.87	-5.00	6.03	****	1.6676	.2443	-.2581	.0281	-.0127	.1124	6.83	.608	
.090	11.87	-5.00	7.95	****	1.8657	.2592	-.3796	.0333	-.0128	.1195	7.12	.612	
.090	11.76	-5.00	9.95	****	2.0672	.2914	-.5033	.0308	-.0142	.1142	7.10	.616	
.090	11.76	-5.00	11.96	****	2.2124	.3150	-.6312	.0371	-.0136	.1232	7.02	.620	
.090	11.76	-5.00	14.02	****	2.4428	.3440	-.7596	.0312	-.0162	.1286	7.10	.625	
.090	11.75	-5.00	15.96	****	2.4825	.4183	-.8914	.0252	-.0195	.1424	5.93	.629	
.092	12.21	-5.00	17.99	****	2.4445	.4742	-.8796	.0305	-.0179	.1369	5.16	.633	
.092	12.21	-5.00	19.90	****	2.4345	.5382	-.8969	.0407	-.0095	.1391	4.52	.638	

LONGITUDINAL STABILITY AXIS AND LATERAL BODY AXIS DATA												TEST NUMBER 284	
MACH	Q, PSF	RETA, DEG	ALPHA, DEG	J	CL	CD	CPM	CRM	CYM	CSF	L/D	H/B	
.094	12.77	5.00	-4.94	****	-.0717	.1679	.6442	.0118	.0181	-.1436	-1.43	.587	
.091	11.98	5.00	-2.99	****	.3883	.1845	.3935	.0076	.0162	-.1213	2.11	.591	
.090	11.87	5.00	-1.99	****	.7674	.1635	.1871	-.0054	.0157	-.1105	4.69	.594	
.090	11.87	5.00	.16	****	.9181	.1647	.1100	-.0128	.0140	-.1081	5.57	.596	
.090	11.87	5.00	1.01	****	1.0096	.1979	.0403	-.0037	.0192	-.1179	5.10	.598	
.090	11.87	5.00	2.08	****	1.2218	.1782	-.0182	-.0068	.0157	-.1118	6.86	.600	
.090	11.75	5.00	2.89	****	1.2989	.2178	-.0429	-.0086	.0163	-.1067	5.96	.602	
.090	11.75	5.00	4.00	****	1.4122	.2109	-.1725	-.0120	.0176	-.1091	6.70	.604	
.089	11.64	5.00	6.11	****	1.6799	.2320	-.3708	-.0158	.0141	-.1025	7.24	.608	
.091	12.09	5.00	8.06	****	1.8527	.2418	-.4233	.0207	.0138	-.0938	7.66	.612	
.091	11.98	5.00	10.10	****	2.0322	.2897	-.5163	-.0197	.0166	-.1046	7.02	.616	
.092	12.32	5.00	11.92	****	2.2339	.3073	-.6511	-.0224	.0161	-.0924	7.27	.620	
.092	12.21	5.00	14.12	****	2.3578	.3496	-.7503	-.0310	.0188	-.1023	6.74	.625	
.092	12.21	5.00	15.99	****	2.4131	.4062	-.8198	-.0354	.0064	-.0862	5.94	.629	
.091	12.09	5.00	18.11	****	2.4554	.4691	-.9137	-.0415	.0059	-.0928	5.23	.634	
.092	12.21	5.00	20.05	****	2.3772	.5609	-.8886	-.0302	.0030	-.0881	4.24	.638	

RUN NUMBER 377		LONGITUDINAL STABILITY AXIS AND LATERAL BODY AXIS DATA										TEST NUMBER 284	
MACH	Q,PSF	BETA,DEG	ALPHA,DEG	J	CL	CD	CPM	CRM	CYM	CSF	L/D	H/B	
.091	12.09	-.02	-4.97	****	.0417	.1857	.5088	.0082	-.0062	.0045	.22	.587	
.091	12.09	-.02	-2.99	****	.4034	.1746	.3118	-.0068	-.0037	.0293	2.31	.591	
.090	11.98	-.02	-.88	****	.7897	.1842	.1254	.0064	-.0042	.0221	4.29	.594	
.090	11.87	-.02	-.06	****	.9169	.2144	.0408	.0005	-.0067	.0177	4.28	.596	
.090	11.98	-.02	1.08	****	1.0886	.2072	-.0483	.0037	-.0075	.0227	5.25	.598	
.091	12.09	-.02	2.08	****	1.2417	.2190	-.1151	.0041	-.0056	.0117	5.67	.600	
.090	11.98	-.02	3.19	****	1.4086	.2198	-.1790	-.0045	-.0097	.0278	6.41	.602	
.091	12.21	-.02	3.89	****	1.4867	.2395	-.2317	.0091	-.0035	.0180	6.21	.604	
.091	12.21	-.02	5.96	****	1.7253	.2523	-.3649	.0060	-.0060	.0284	6.84	.608	
.091	12.21	-.02	8.10	****	1.8997	.2615	-.4825	.0105	-.0015	.0177	7.27	.612	
.091	12.09	-.02	10.06	****	2.0704	.3072	-.5620	.0096	.0021	.0067	6.74	.616	
.091	12.21	-.02	11.81	****	2.2286	.3350	-.6411	.0027	-.0022	.0094	6.65	.620	
.090	11.98	-.02	13.97	****	2.3629	.3770	-.7388	-.0016	-.0061	.0083	6.27	.625	
.090	11.98	-.02	15.96	****	2.4043	.4223	-.7908	-.0113	-.0131	.0230	5.69	.629	
.090	11.98	-.02	18.03	****	2.4075	.5014	-.8500	-.0073	-.0124	.0106	4.80	.634	
.090	11.75	-.02	20.09	****	2.4061	.5701	-.8556	-.0006	-.0056	.0039	4.22	.638	

RUN NUMBER 380		LONGITUDINAL STABILITY AXIS AND LATERAL BODY AXIS DATA										TEST NUMBER 284	
MACH	Q,PSF	BETA,DFG	ALPHA,DEG	J	CL	CD	CPM	CRM	CYM	CSF	L/D	H/B	
.090	11.98	-.05	-4.94	****	.1900	.2005	.2732	-.0106	-.0025	.0269	.95	.587	
.091	12.09	-.05	-2.99	****	.4450	.1948	.1471	-.0026	-.0087	.0332	2.28	.590	
.090	11.98	-.05	-1.03	****	.8741	.2097	-.0437	.0039	-.0070	.0340	4.17	.594	
.090	11.98	-.05	.09	****	.9811	.2086	-.0816	.0000	-.0060	.0182	4.70	.596	
.091	12.09	-.05	1.08	****	1.1202	.2136	-.1573	.0040	-.0068	.0262	5.24	.598	
.090	11.87	-.05	2.12	****	1.2484	.2267	-.1987	.0040	-.0051	.0236	5.51	.600	
.090	11.87	-.05	3.08	****	1.4379	.2336	-.2618	-.0022	-.0078	.0320	6.16	.602	
.090	11.87	-.05	3.93	****	1.5005	.2548	-.3183	.0114	-.0023	.0167	5.89	.603	
.089	11.75	-.05	6.18	****	1.7209	.2652	-.3935	.0079	-.0027	.0181	6.49	.608	
.090	11.87	-.05	8.14	****	1.8880	.2894	-.4627	.0008	-.0054	.0266	6.55	.612	
.090	11.87	-.05	9.99	****	2.0479	.3274	-.5254	.0042	-.0044	.0276	6.26	.616	
.089	11.76	-.05	11.96	****	2.2615	.3550	-.6163	.0026	-.0030	.0144	6.37	.620	
.090	11.87	-.05	14.23	****	2.3672	.4029	-.6982	-.0002	-.0063	.0215	5.88	.625	
.089	11.75	-.05	15.99	****	2.3912	.4290	-.7366	-.0057	-.0106	.0187	5.57	.629	
.090	11.76	-.05	17.73	****	2.3721	.4963	-.7741	-.0054	-.0080	.0212	4.78	.633	
.089	11.64	-.05	20.05	****	2.3313	.5907	-.7242	.0099	.0012	.0007	3.95	.638	

RUN NUMBER 383		LONGITUDINAL STABILITY AXIS AND LATERAL BODY AXIS DATA										TEST NUMBER 284	
MACH	Q,PSF	BETA,DEG	ALPHA,DEG	J	CL	CD	CPM	CRM	CYM	CSF	L/D	H/B	
.090	11.98	.03	-4.97	****	.3980	.1814	-.4771	-.0041	-.0011	.0172	2.19	.590	
.090	11.98	.03	-3.03	****	.7104	.1922	-.5395	-.0146	-.0028	.0130	3.70	.593	
.091	12.09	.03	-.99	****	1.0458	.1977	-.6129	.0026	-.0046	.0183	5.29	.597	
.090	11.98	.03	-.06	****	1.1213	.2157	-.6193	-.0063	-.0063	.0173	5.20	.599	
.090	11.98	.03	1.08	****	1.2942	.2175	-.6164	-.0044	-.0041	.0151	5.95	.601	
.090	11.87	.03	2.16	****	1.4336	.2209	-.6077	.0044	-.0036	.0120	6.49	.603	
.090	11.87	.03	3.08	****	1.5381	.2303	-.5985	-.0002	-.0041	.0095	6.68	.605	
.090	11.87	.03	3.97	****	1.6061	.2515	-.5925	.0055	-.0028	.0096	6.39	.606	
.089	11.75	.03	6.14	****	1.7912	.2678	-.5402	-.0015	-.0050	.0122	6.69	.611	
.093	12.77	.03	7.95	****	1.9037	.2897	-.5172	.0078	.0000	.0059	6.57	.614	
.093	12.77	.03	10.32	****	2.0986	.3205	-.4508	.0028	-.0034	.0120	6.98	.619	
.094	12.88	.03	12.03	****	2.1919	.3246	-.4061	-.0003	-.0040	.0095	6.75	.623	
.092	12.43	.03	13.78	****	2.3019	.3528	-.3301	-.0025	-.0009	-.0039	6.53	.627	
.090	11.98	.03	15.99	****	2.2810	.3903	-.2399	-.0035	-.0085	.0144	5.84	.632	
.090	11.87	.03	18.03	****	2.2665	.4697	-.1793	-.0055	-.0114	.0153	4.83	.636	
.090	11.98	.03	19.98	****	2.2292	.5321	-.1017	.0017	-.0045	.0070	4.19	.640	

TABLE I. MODEL GEOMETRIC CHARACTERISTICS

Fuselage:	
Body station of fuselage nose, in.	-2.715
Length, ft	11.99
Maximum diameter, in.	13.8
Supercritical wing: ^a	
Area (trapezoidal reference), ft ²	11.21
Area (wetted), ft ²	10.31
Span, ft	10.59
Quarter-chord sweep, deg	27
Aspect ratio	10
Taper ratio (trapezoidal reference)	0.412
Reference geometric chord, in.	13.44
Dihedral, deg	5
Root incidence, deg	-1
Body station of wing leading edge at root, ft	5.01
Body station of moment reference center, ft	6.54
Side-of-body airfoil ($\eta = 0.109$):	
Chord, in.	22.14
(t/c) _{max}	0.144
Twist, deg	2.5
Trailing-edge break airfoil ($\eta = 0.434$):	
Chord, in.	13.4
(t/c) _{max}	0.12
Twist, deg	0.5
Tip airfoil ($\eta = 1.0$):	
Chord, in.	7.41
(t/c) _{max}	0.107
Twist, deg	-0.7
Horizontal tail: ^a	
Area, ft ²	4.5
Span, ft	4.14
Aspect ratio	3.78
Quarter-chord sweep, deg	35
Dihedral, deg	10
Taper ratio	0.36
Mean geometric chord, in.	14.0
Body station of tail leading edge at root, ft	14
Root airfoil:	
Chord, in.	19.2
(t/c) _{max}	0.095
Tip airfoil (symmetric):	
Chord, in.	7.0
(t/c) _{max}	0.085

^aDihedral not included in span and area dimensions.

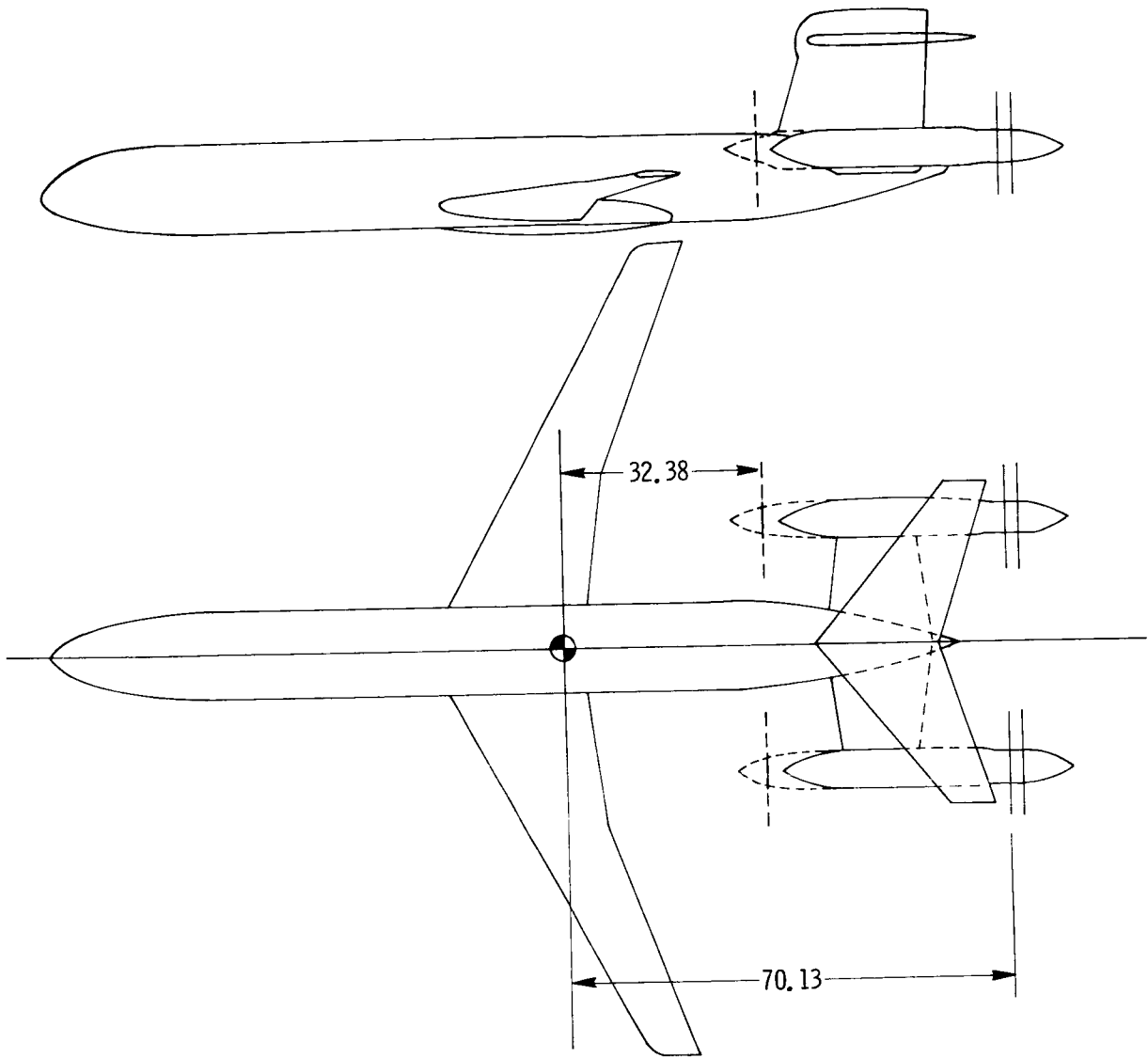
TABLE I. Concluded

Vertical tail:	
Area, ft ²	2.82
Height, in.	19.05
Leading-edge sweep, deg	15.75
Body station of tail leading edge at root, ft	9.43
Root airfoil:	
Chord, in.	23.42
(t/c) _{max}	0.12
Tip airfoil:	
Chord, in.	19.21
(t/c) _{max}	0.12
Pylon: ^a	
Area (trapezoidal reference), ft ²	3.8
Span, ft	2.89
Aspect ratio	2.2
Quarter-chord sweep, deg	6.0
Dihedral, deg	16.1
Taper ratio	0.63
Body station of pylon leading edge at root, ft	9.88
Root airfoil:	
Chord, in.	19.6
(t/c) _{max}	0.12
Side-of-nacelle airfoil:	
Chord, in.	12.4
(t/c) _{max}	0.12
Propellers:	
Single rotation:	
Tip diameter, in.	16.9
Maximum nacelle diameter, in.	6.0
Body station at propeller disk, ft	9.2
Counter rotation:	
Tip diameter, in.	16.1
Spacing between blade disks, in.	2.3
Maximum nacelle diameter, in.	6.0
Body station at forward propeller disk, ft.	12.4

^aDihedral not included in span and area dimensions.

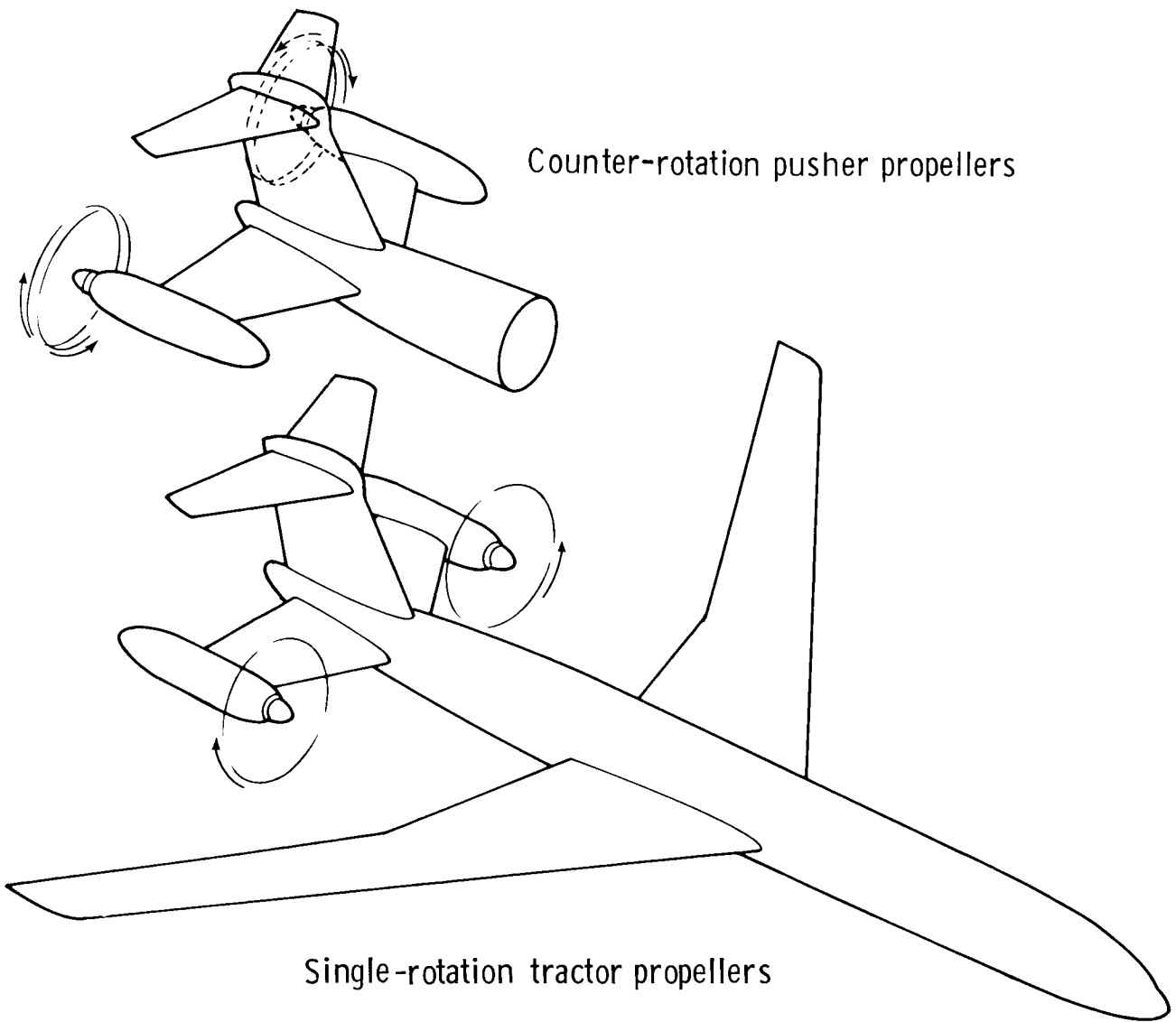
TABLE II. STRAIN-GAUGE BALANCE CHARACTERISTICS

Component	Maximum load	Accuracy
Normal force, lb	3 000	±15
Axial force, lb	500	±2.5
Pitching moment, in-lb	25 000	±125
Rolling moment, in-lb	9 900	±49.5
Yawing moment, lb	10 000	±50
Side force, lb	1 000	±5



(a) Plan view and side view.

Figure 1. Geometric characteristics of model with aft-fuselage-mounted turboprops installed. All dimensions are given in inches.



Counter-rotation pusher propellers

Single-rotation tractor propellers

(b) Isometric sketch of propeller installations.

Figure 1. Concluded.

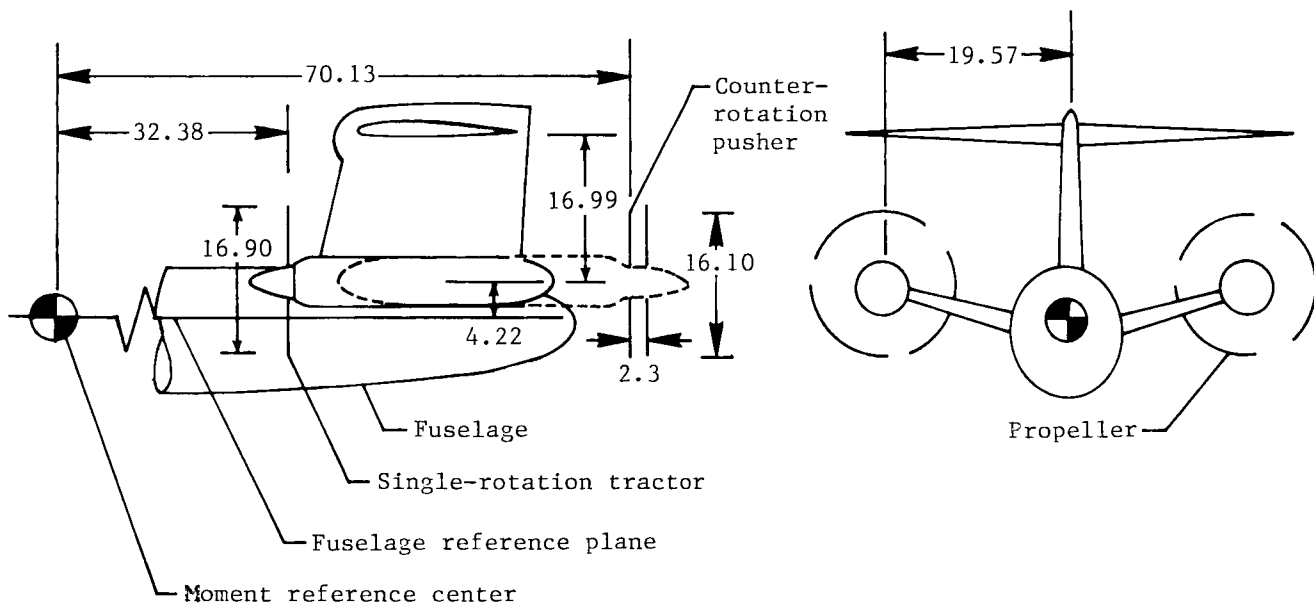


Figure 2. Sketch of modified aft end indicating geometric characteristics of single-rotation tractor and counter-rotation pusher configurations. All dimensions are given in inches.

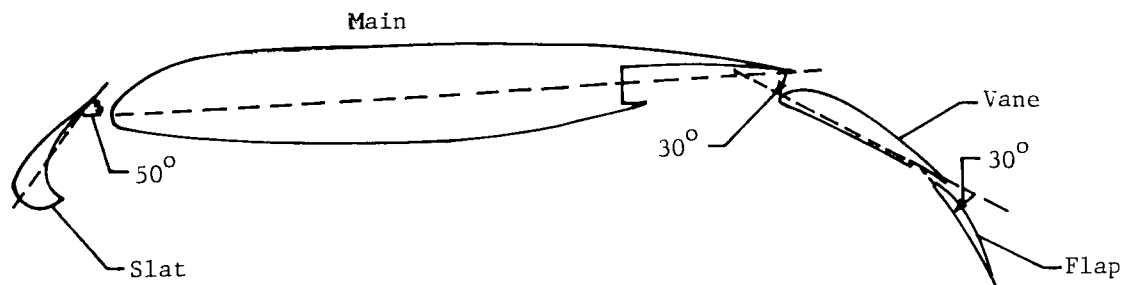
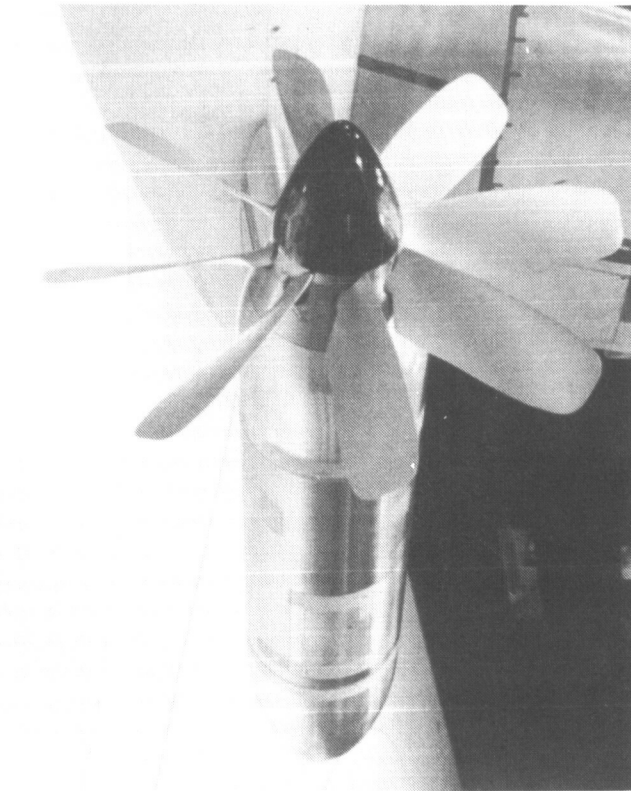
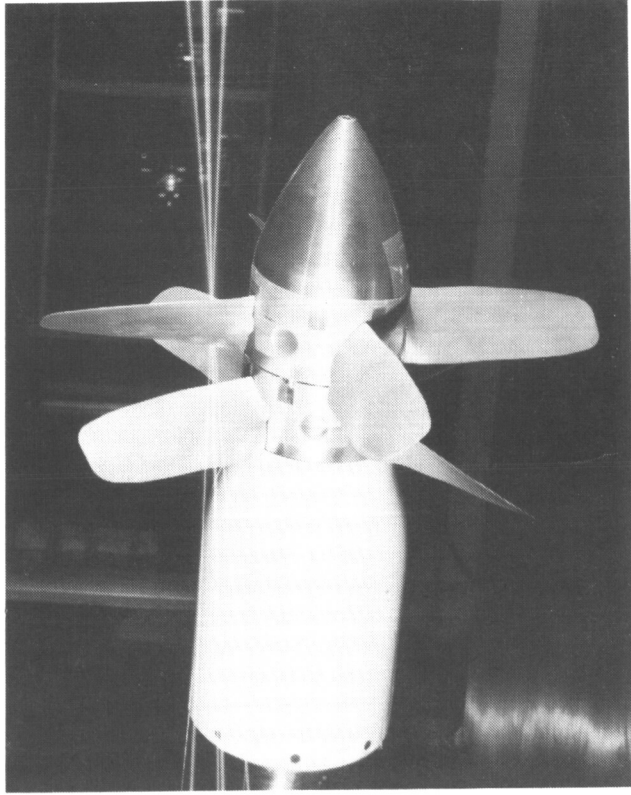


Figure 3. Cross-sectional view of wing and high-lift system.



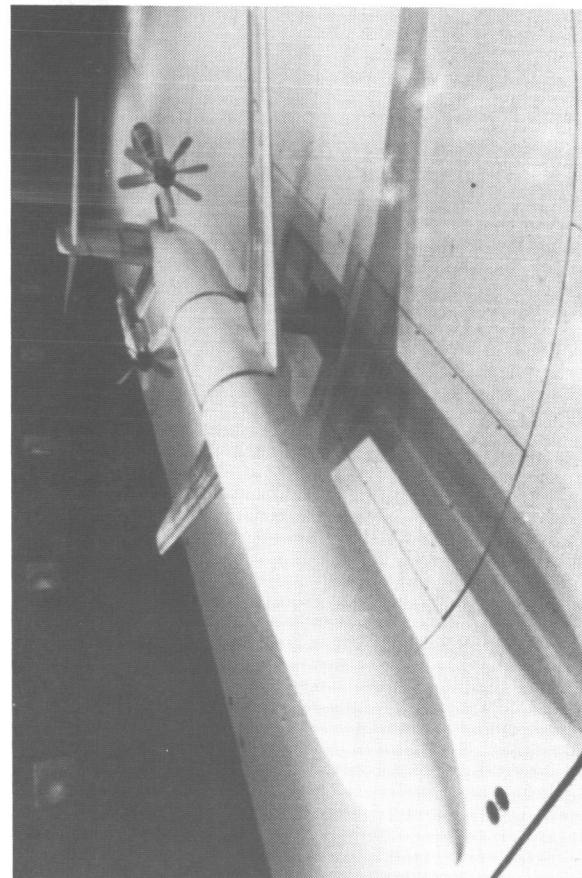
(a) Single-rotation propeller.



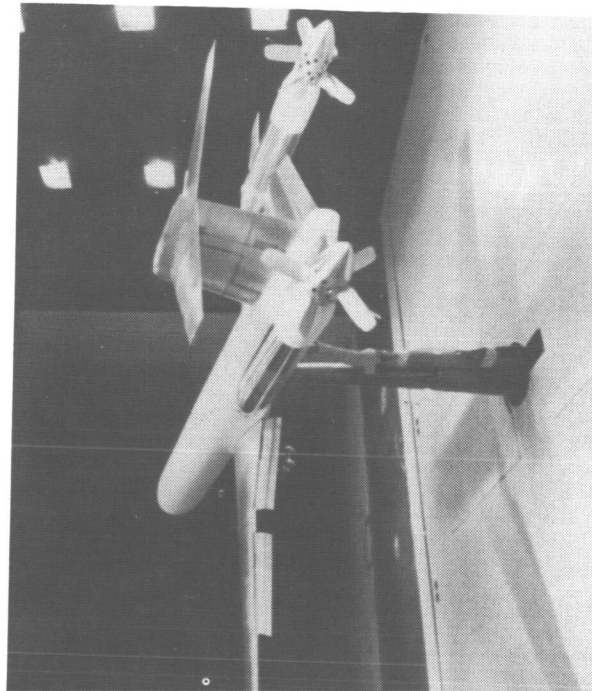
L-85-174

(b) Counter-rotation propeller.

Figure 4. Propeller systems installed in the Langley 4- by 7-Meter Tunnel .



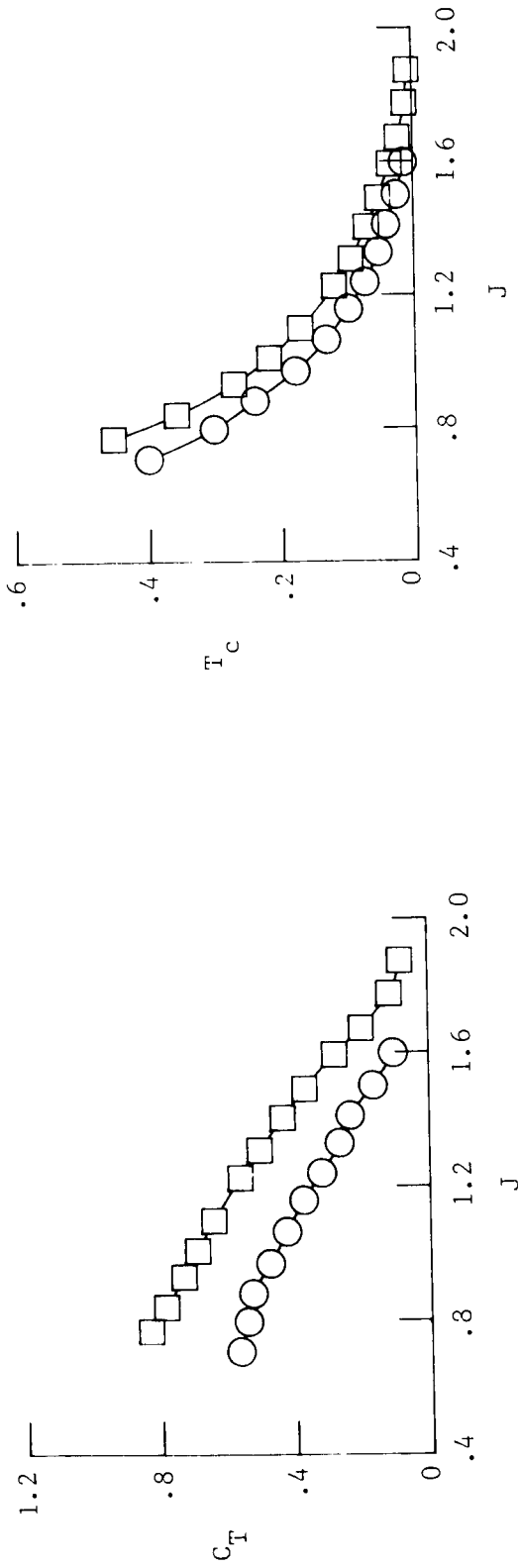
(a) Single-rotation tractor configuration.



(b) Counter-rotation pusher configuration.
L-84-11,276

Figure 5. Model installed in the Langley 4- by 7-Meter Tunnel.

- Eight-blade SF propeller (Blade angle, 40.3°)
- Four-by-four blade CR propeller (Blade angle, $41.3^\circ/41.3^\circ$)



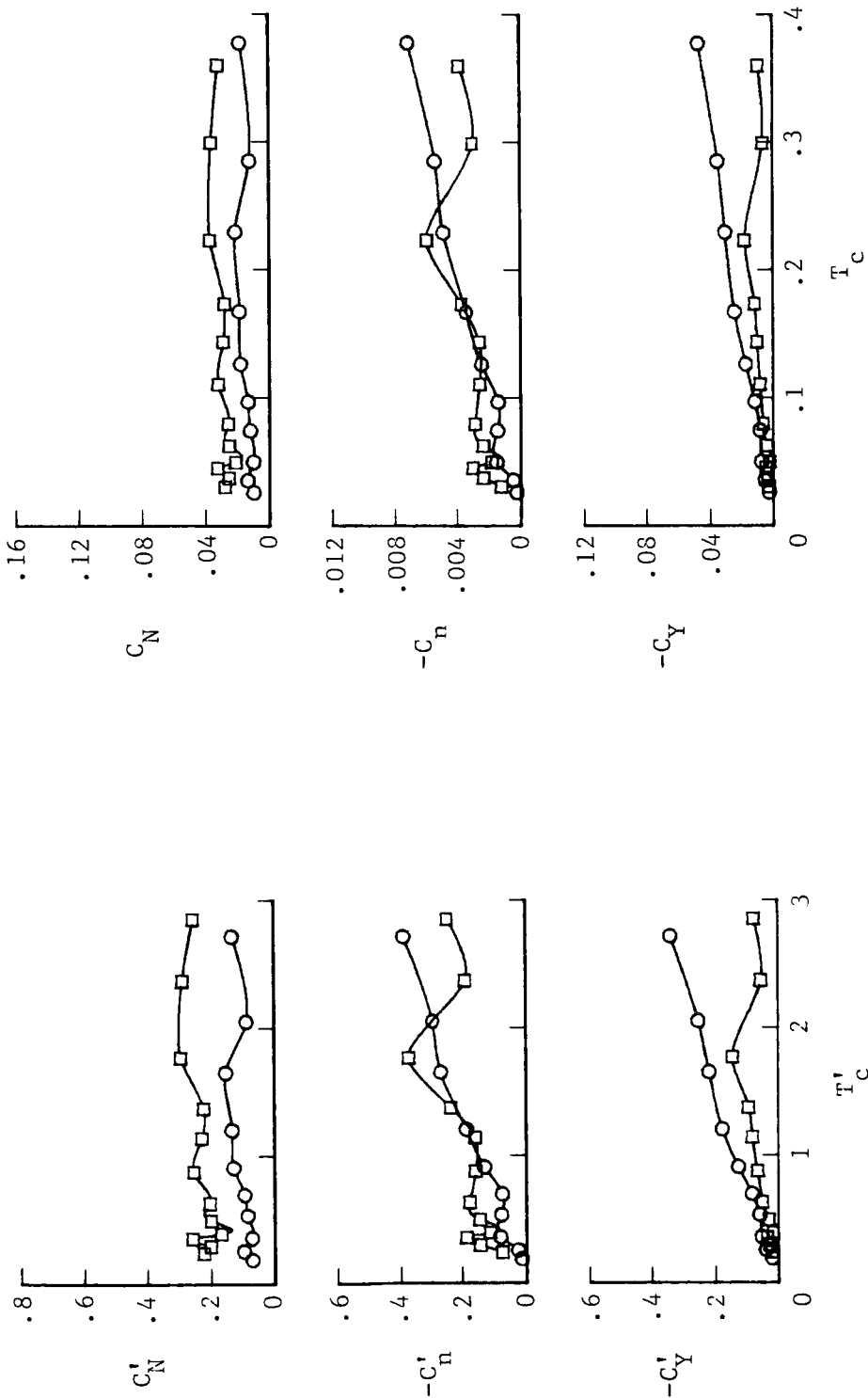
(a) Propeller reference system.

(b) Model reference system.

Figure 6. Variation of thrust coefficient with advance ratio for isolated propeller. $\alpha = 0^\circ$.

○ Eight-blade SR propeller (Blade angle, 40.3°)

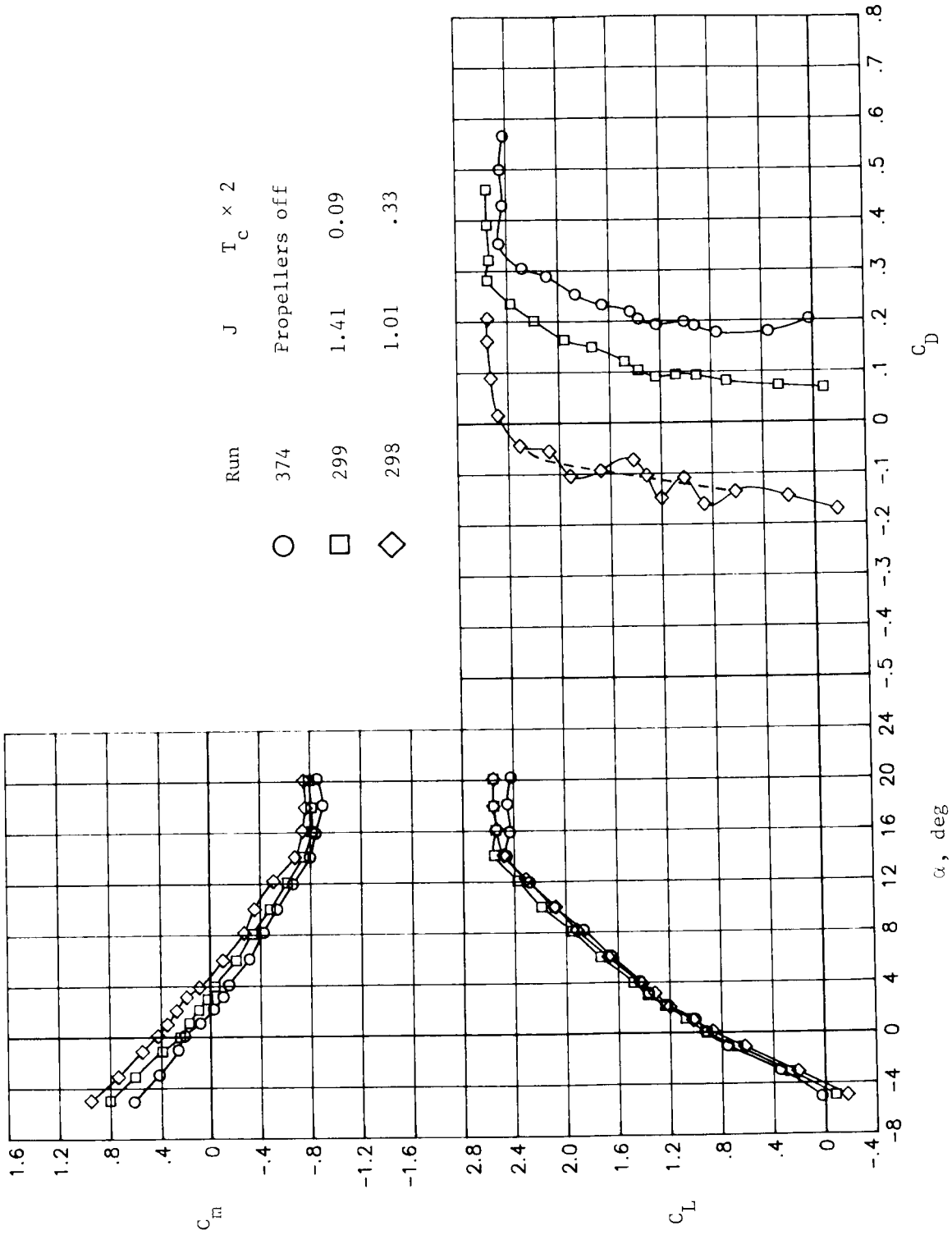
□ Four-by-four blade CR propeller (Blade angle, $41.3^\circ/41.3^\circ$)



(a) Propeller reference system.

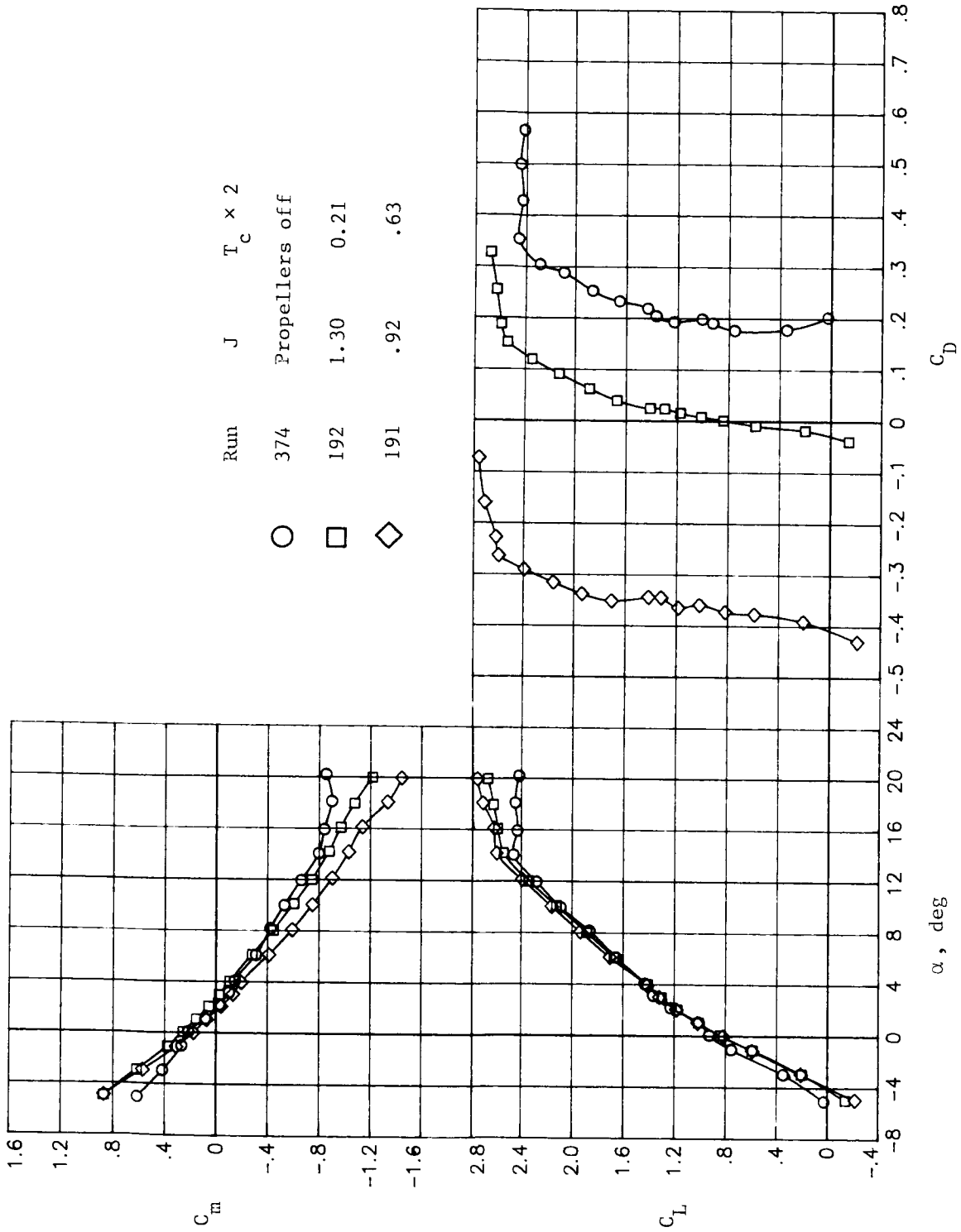
(b) Model reference system.

Figure 7. Isolated propeller characteristics at $\alpha = 10^\circ$.



(a) Single-rotation tractor configuration.

Figure 8. Effect of thrust on longitudinal aerodynamic characteristics.



(b) Counter-rotation pusher configuration.

Figure 8. Concluded.

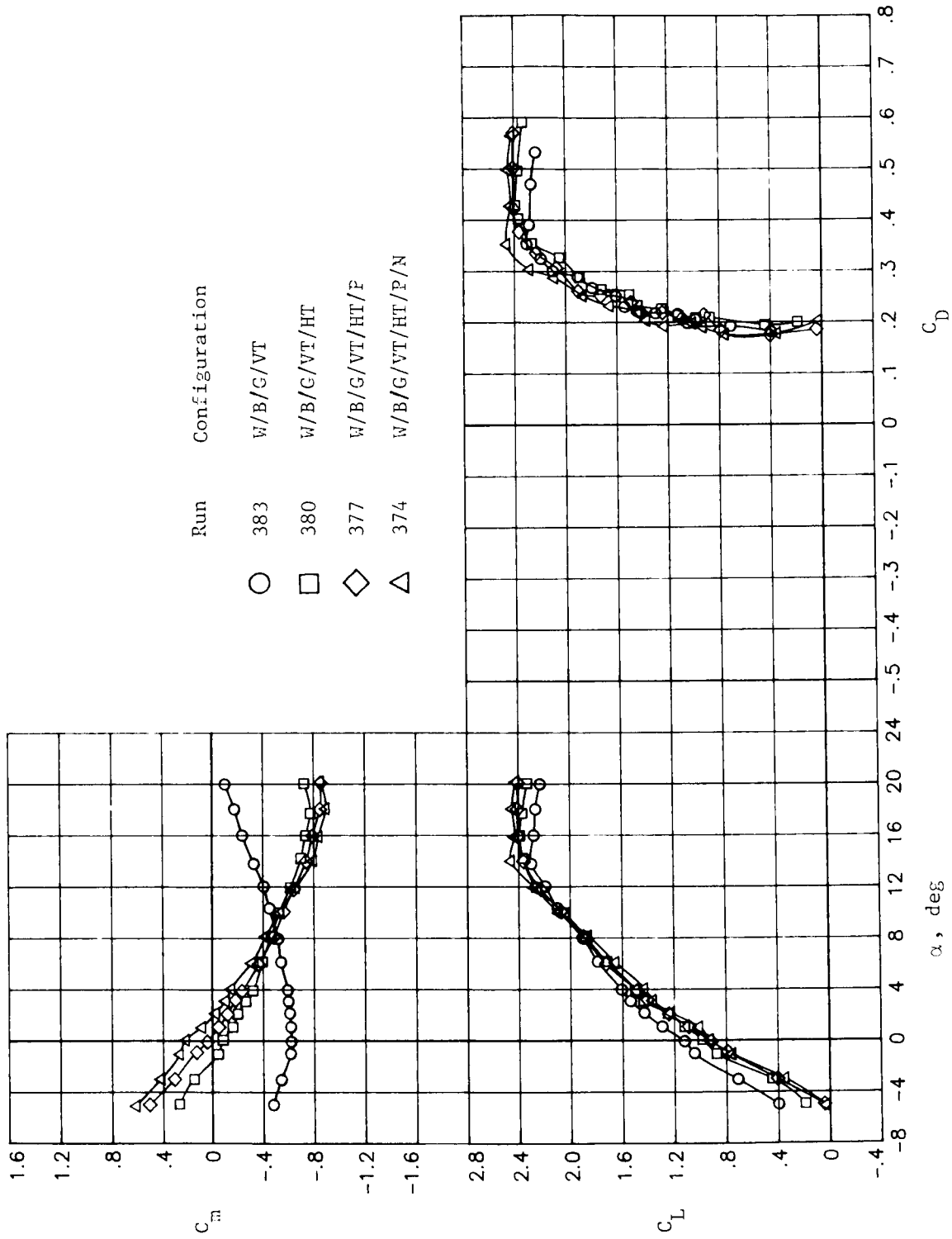
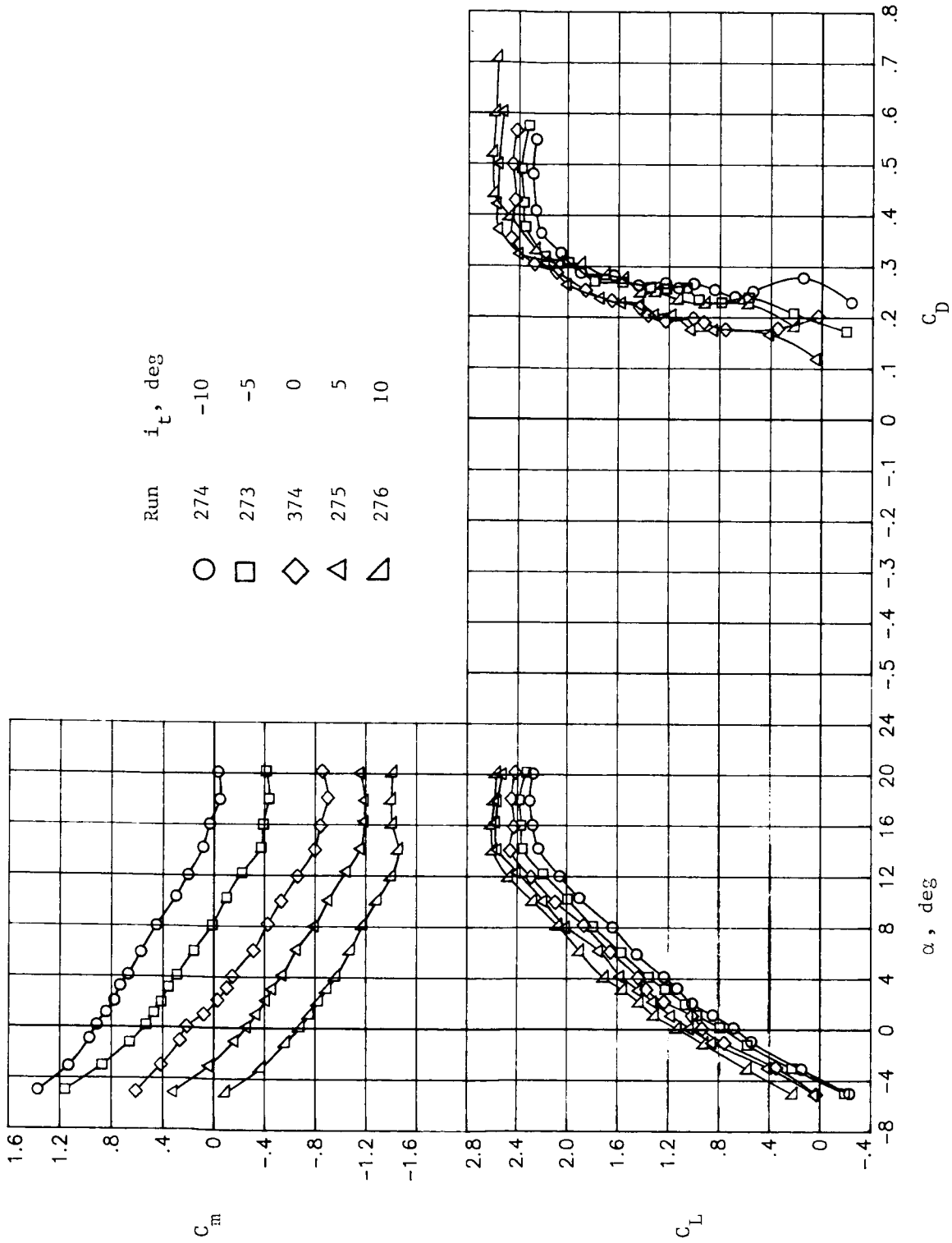
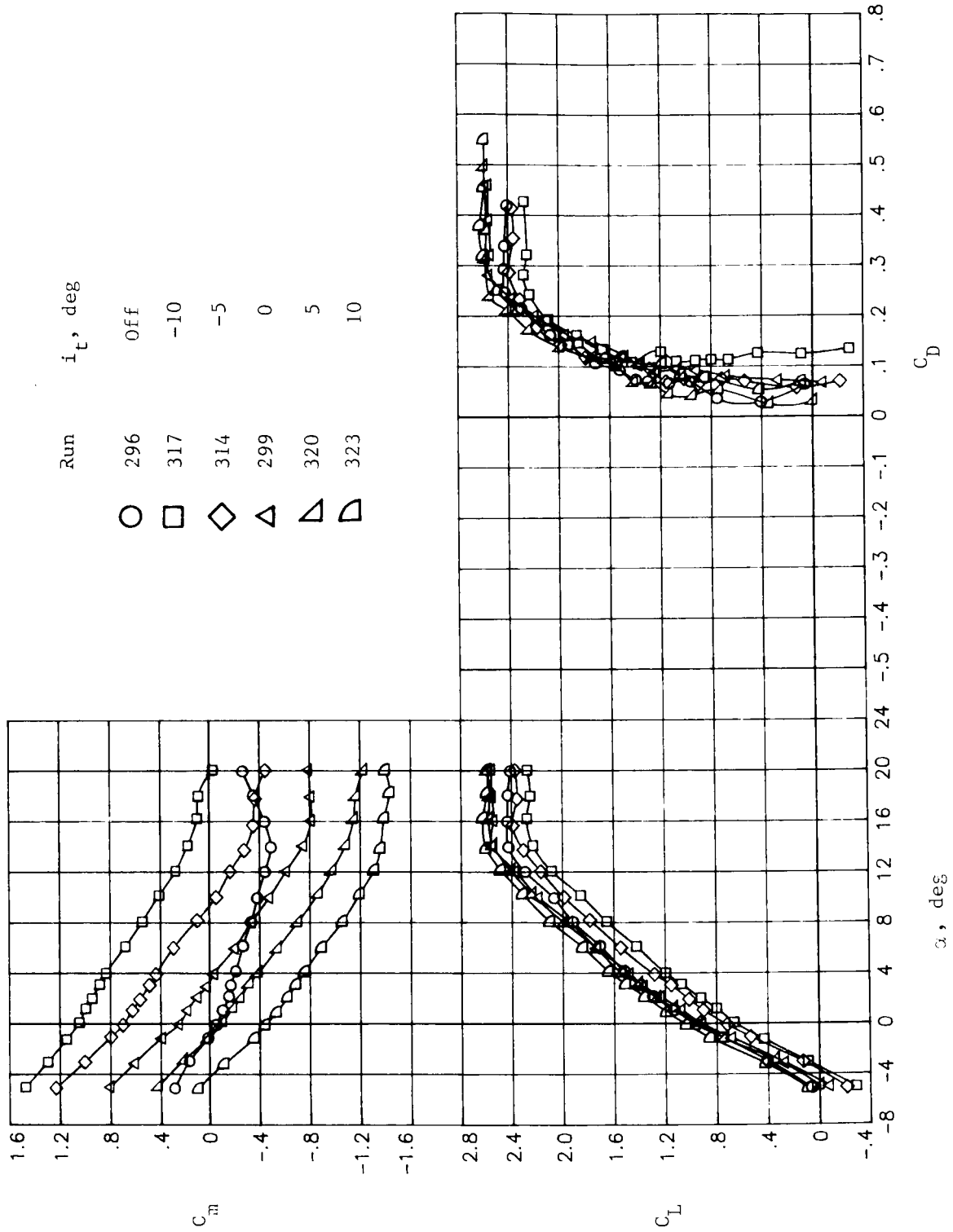


Figure 9. Effect of aft-mounted pylon and nacelles on longitudinal aerodynamic characteristics of unpowered (propellers off) aircraft configuration. $i_t = 0^\circ$.



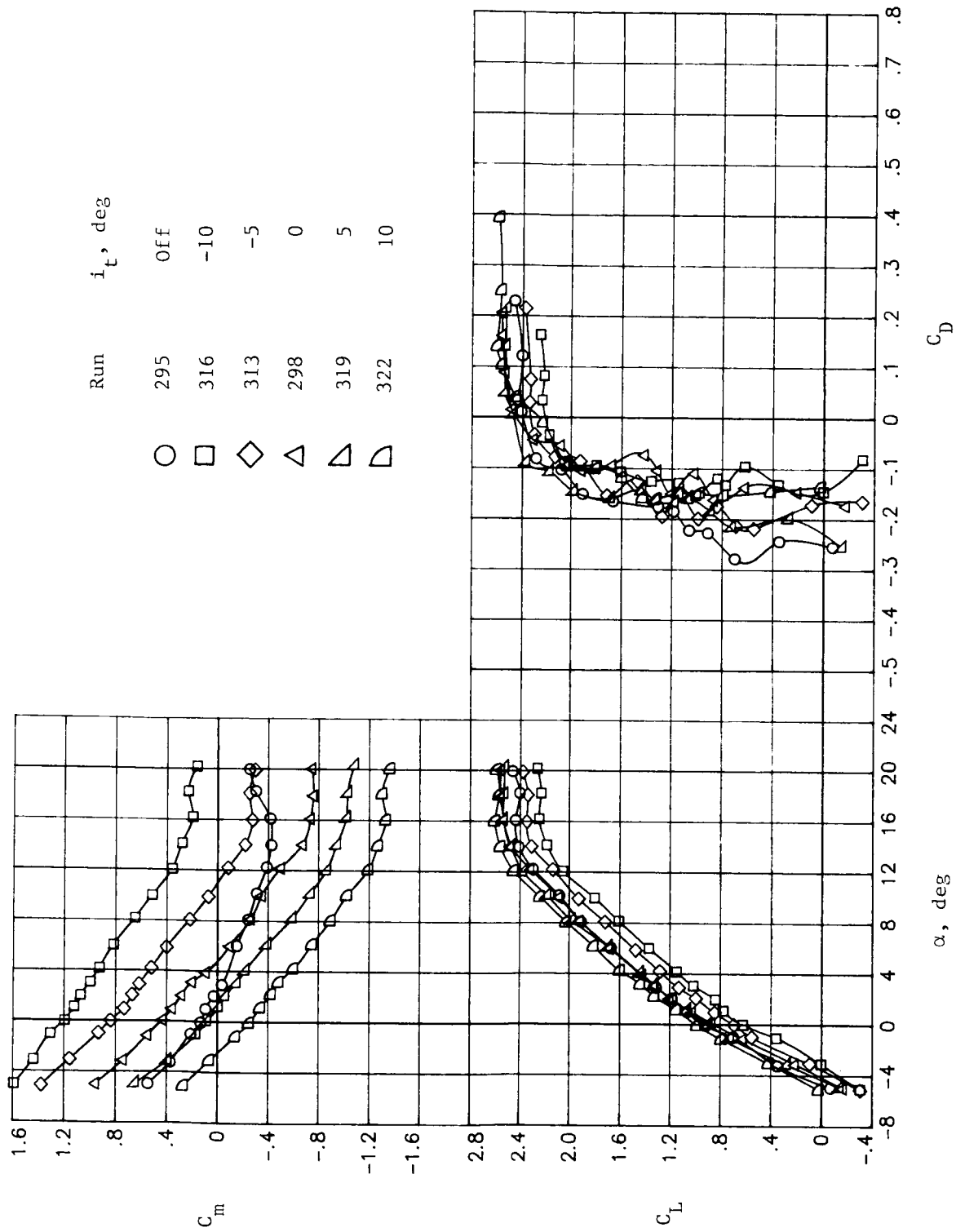
(a) Power off (propellers off).

Figure 10. Effect of horizontal tail deflection on longitudinal aerodynamic characteristics.



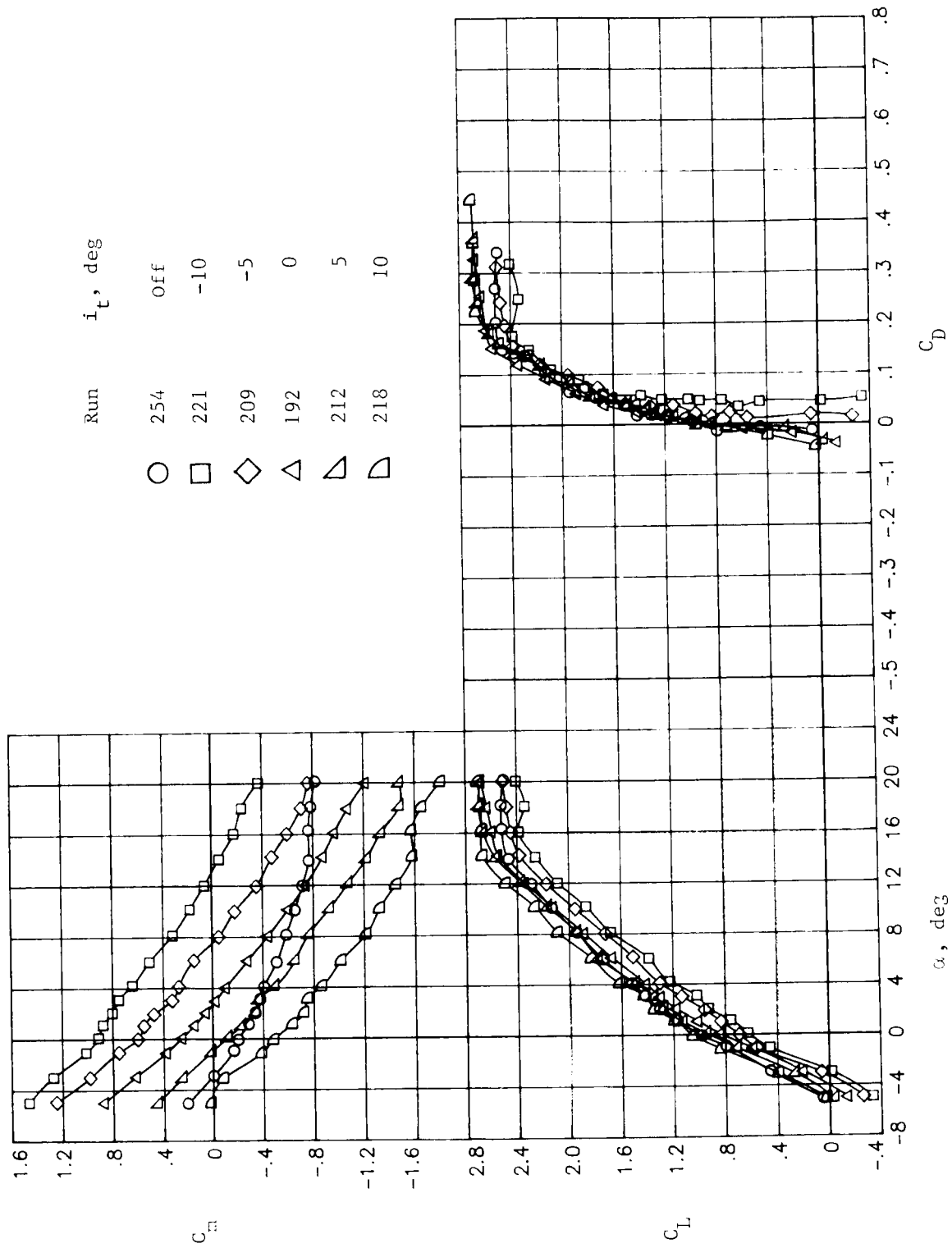
(b) Single-rotation tractor configuration. $J = 1.41$.

Figure 10. Continued.



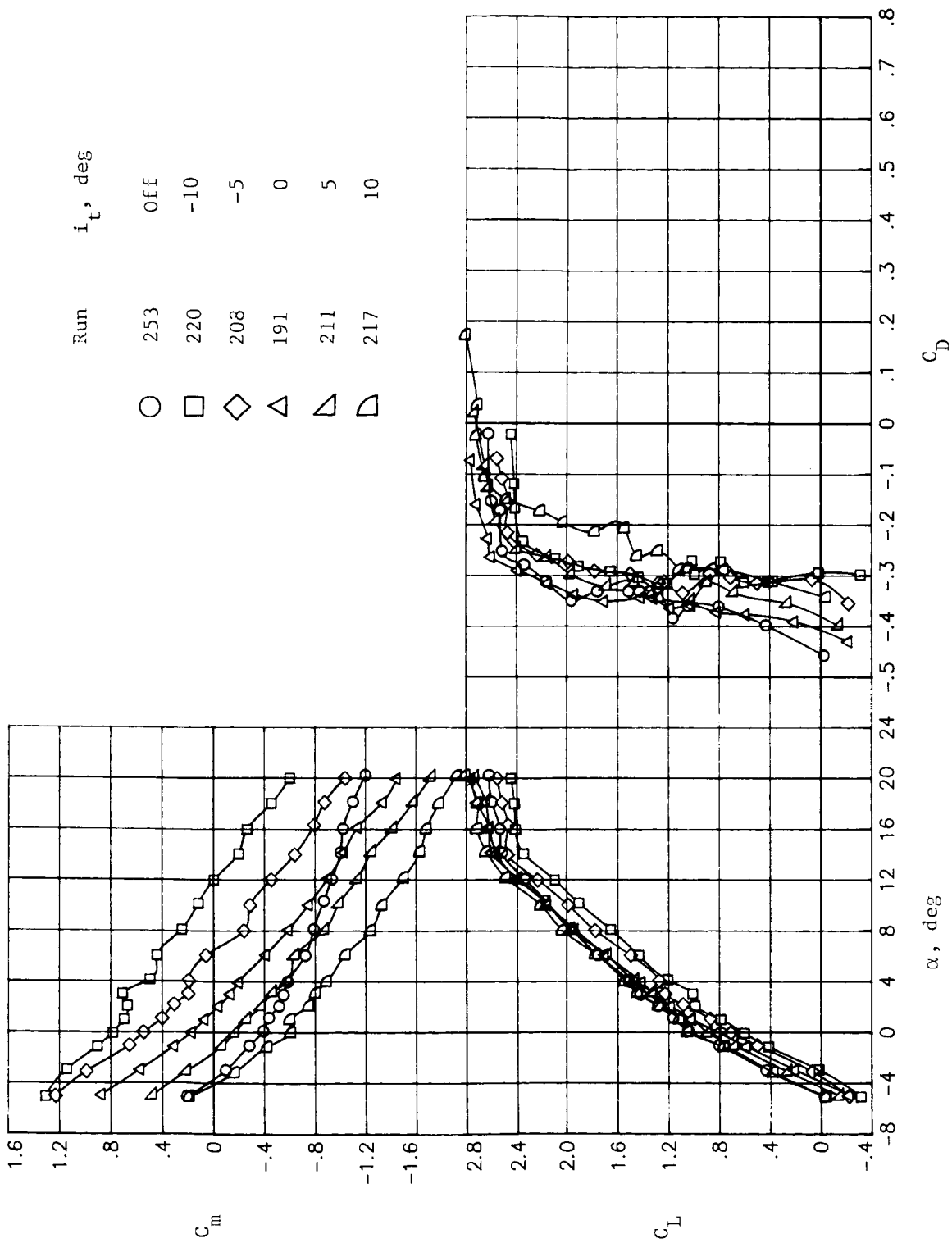
(c) Single-rotation tractor configuration. $J = 1.01$.

Figure 10. Continued.



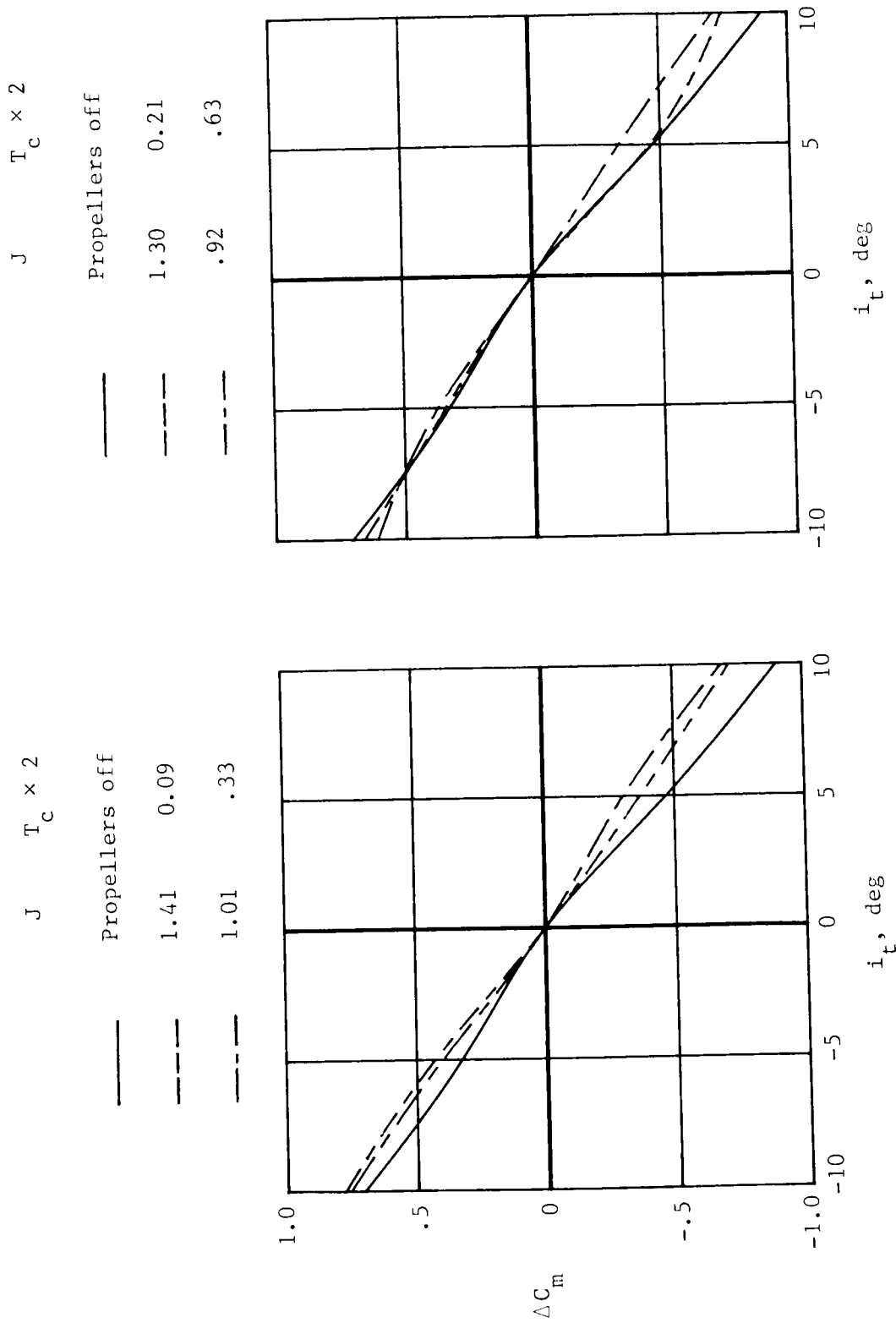
(d) Counter-rotation pusher configuration. $J = 1.30$.

Figure 10. Continued.



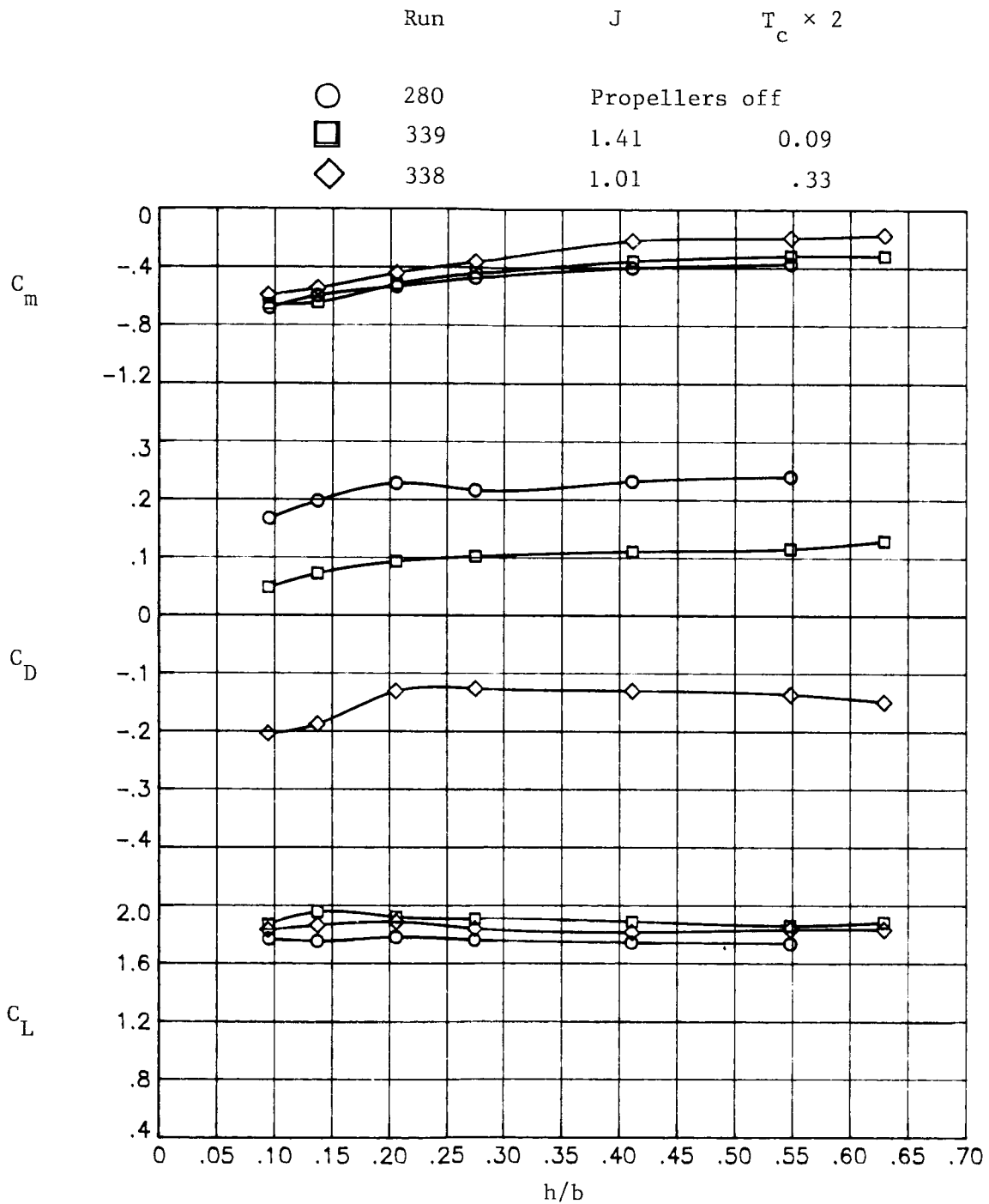
(e) Counter-rotation pusher configuration. $J = 0.92$.

Figure 10. Concluded



(a) Single-rotation tractor configuration. (b) Counter-rotation pusher configuration.

Figure 11. Effect of thrust on horizontal tail control effectiveness. $\alpha = 0^\circ$.

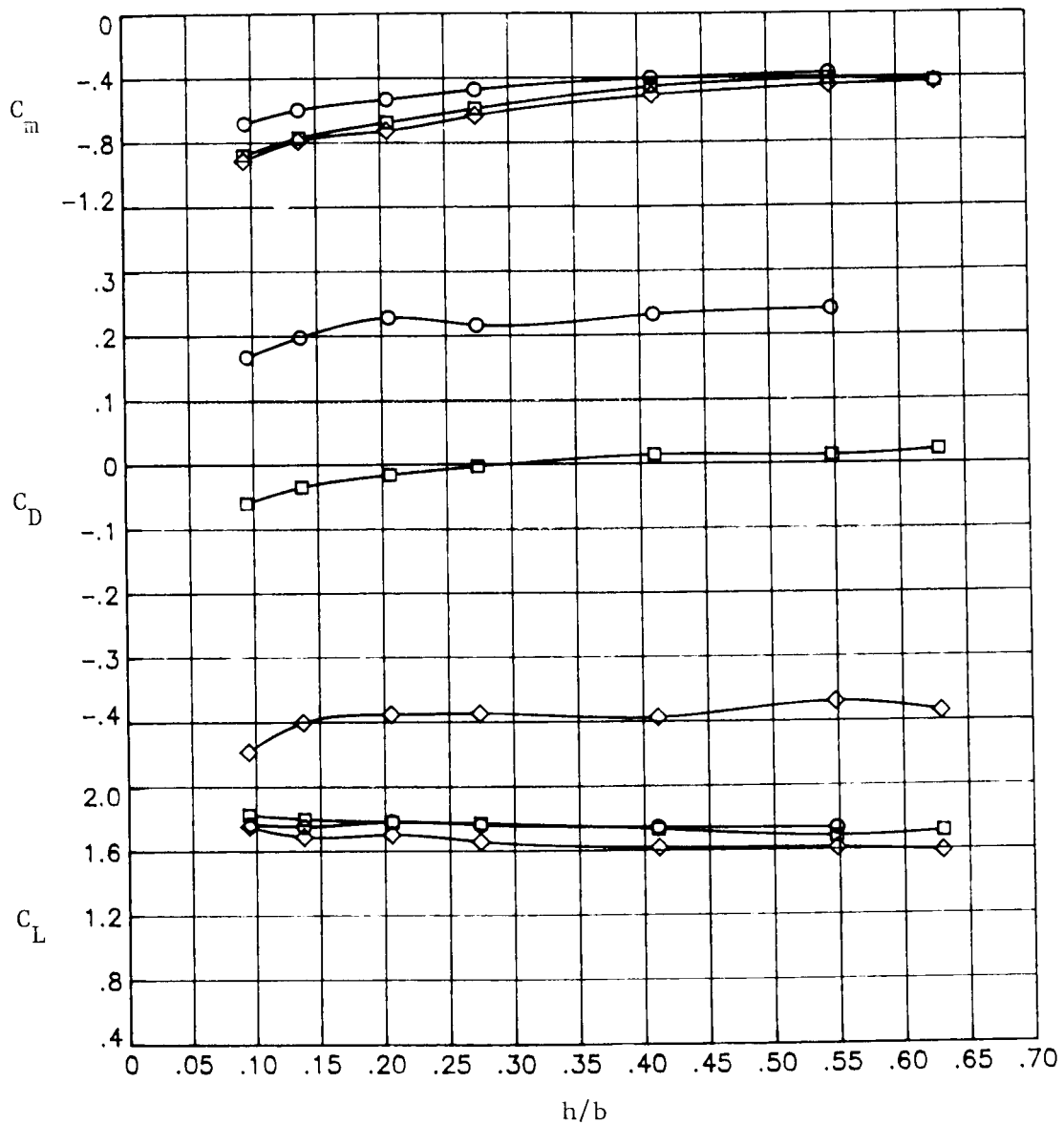


(a) Single-rotation tractor configuration.

Figure 12. Effect of ground height and thrust on longitudinal aerodynamic characteristics. $\alpha = 8^\circ; i_t = 0^\circ$.

Run	J	$T_c \times 2$
-----	---	----------------

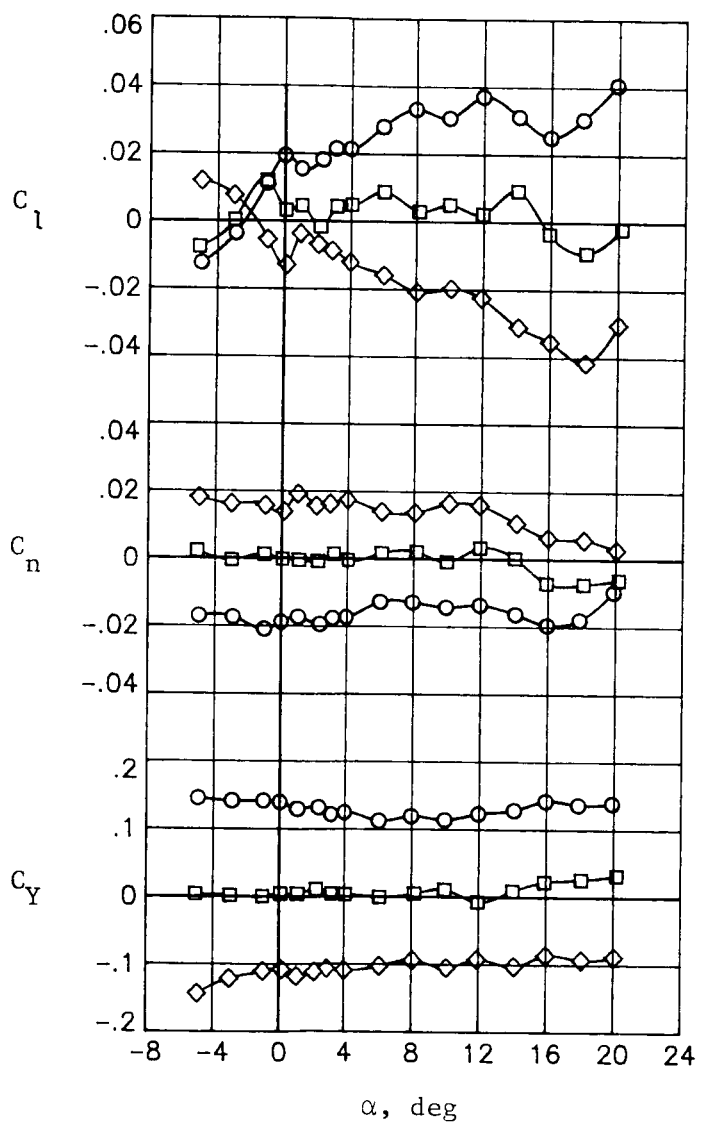
○	280	Propellers off	
□	206	1.30	0.21
◇	205	.92	.63



(b) Counter-rotation pusher configuration.

Figure 12. Concluded.

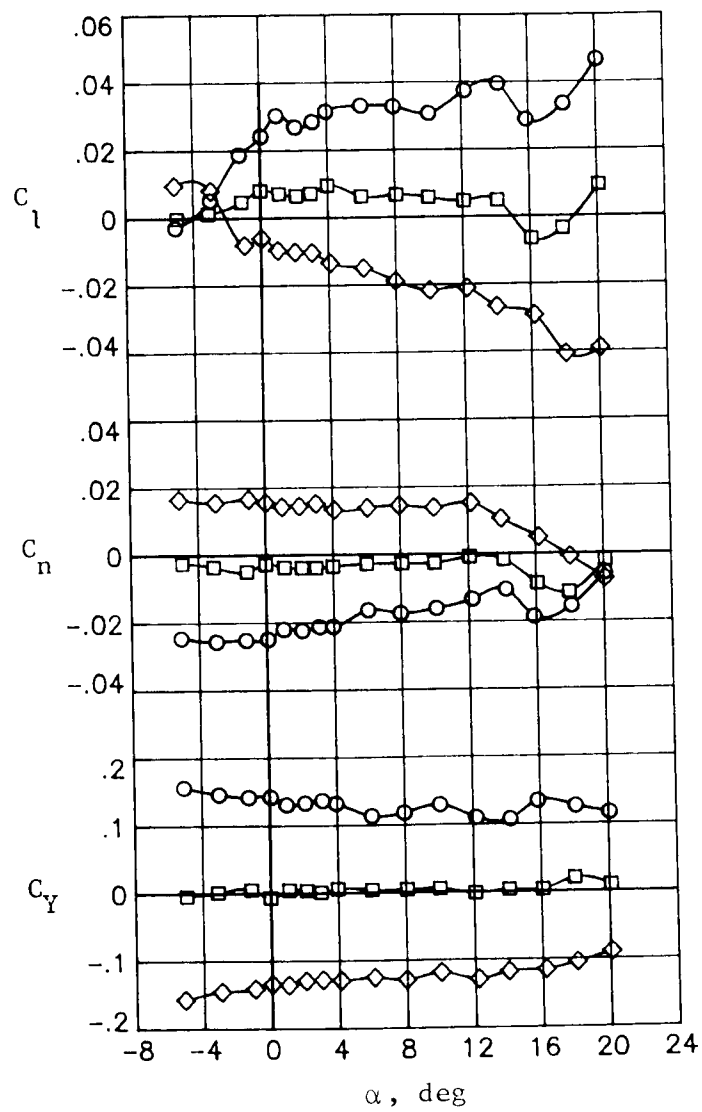
	Run	β , deg
○	375	-5
□	374	0
◇	376	5



(a) Power off (propellers off).

Figure 13. Effect of sideslip on lateral-directional aerodynamic characteristics.

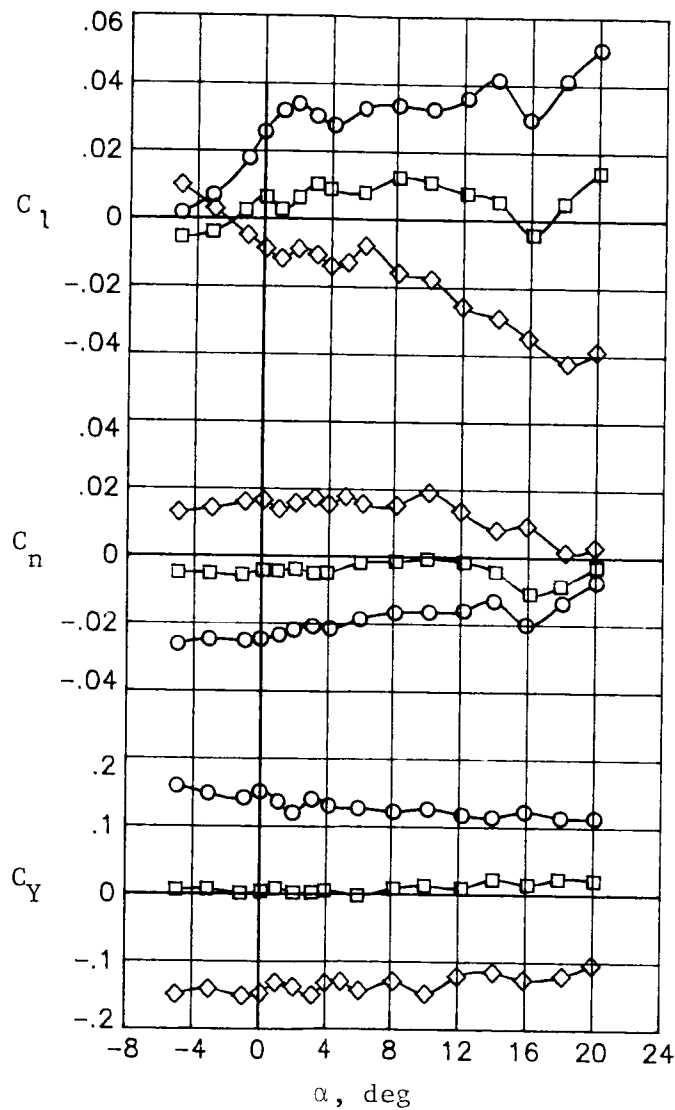
	Run	β , deg
○	305	-5
□	299	0
◇	302	5



(b) Single-rotation tractor configuration. $J = 1.41$.

Figure 13. Continued.

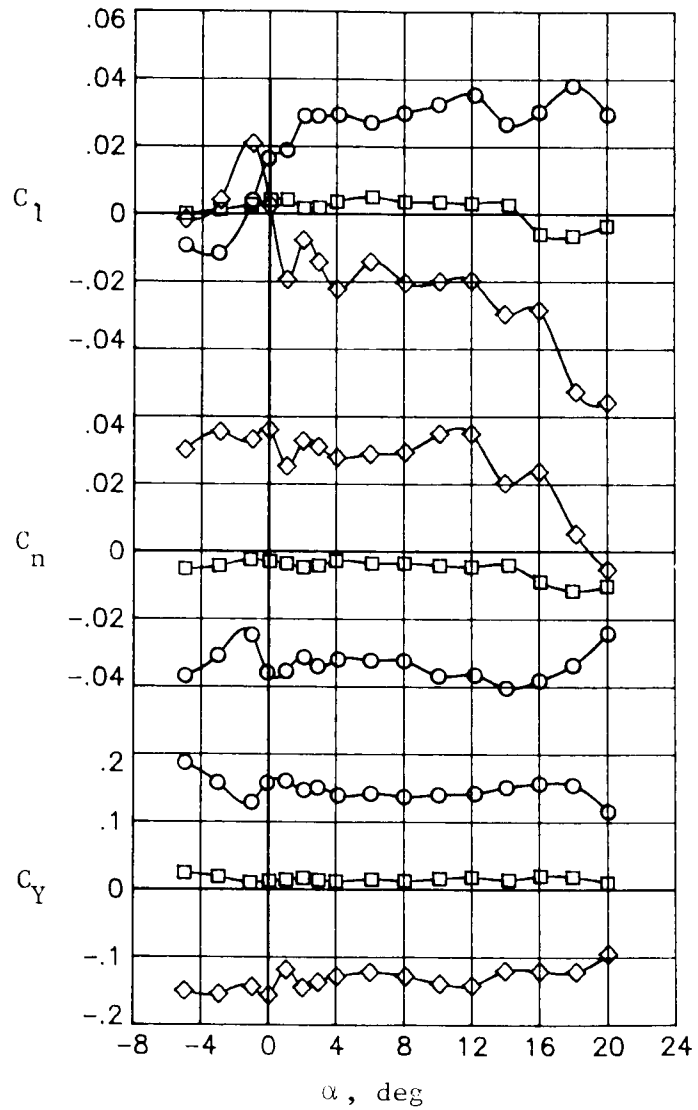
	Run	β , deg
○	304	-5
□	298	0
◇	303	5



(c) Single-rotation tractor configuration. $J = 1.01$.

Figure 13. Continued.

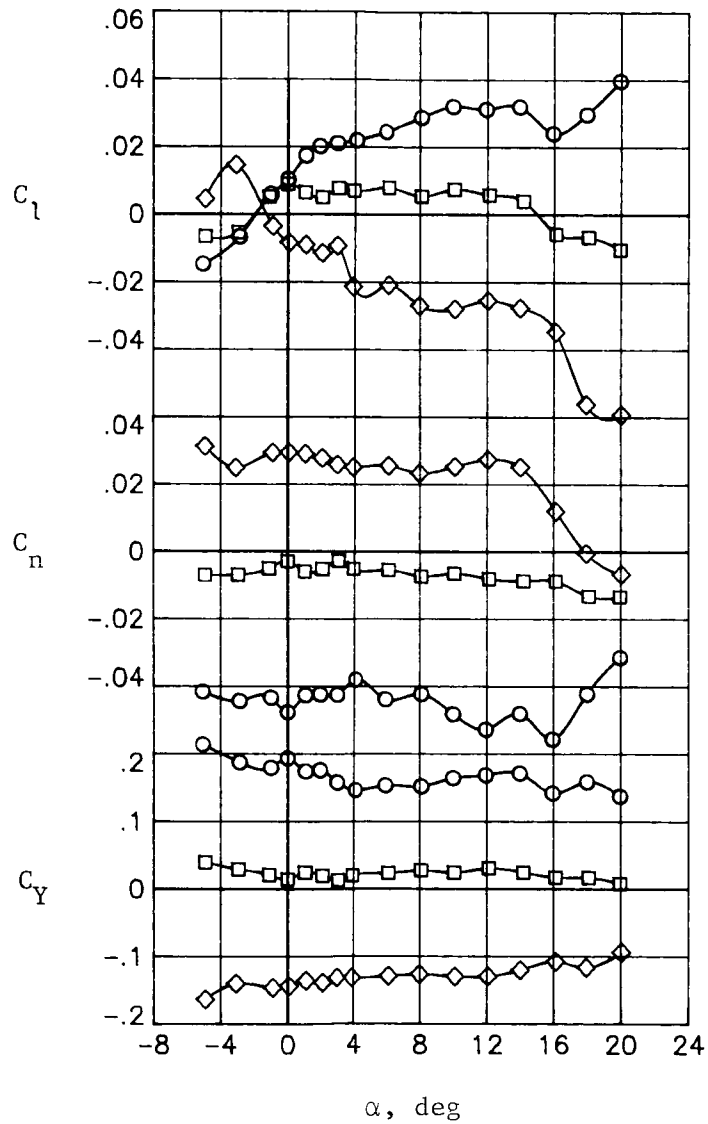
	Run	β , deg
○	198	-5
□	192	0
◇	201	5



(d) Counter-rotation pusher configuration. $J = 1.30$.

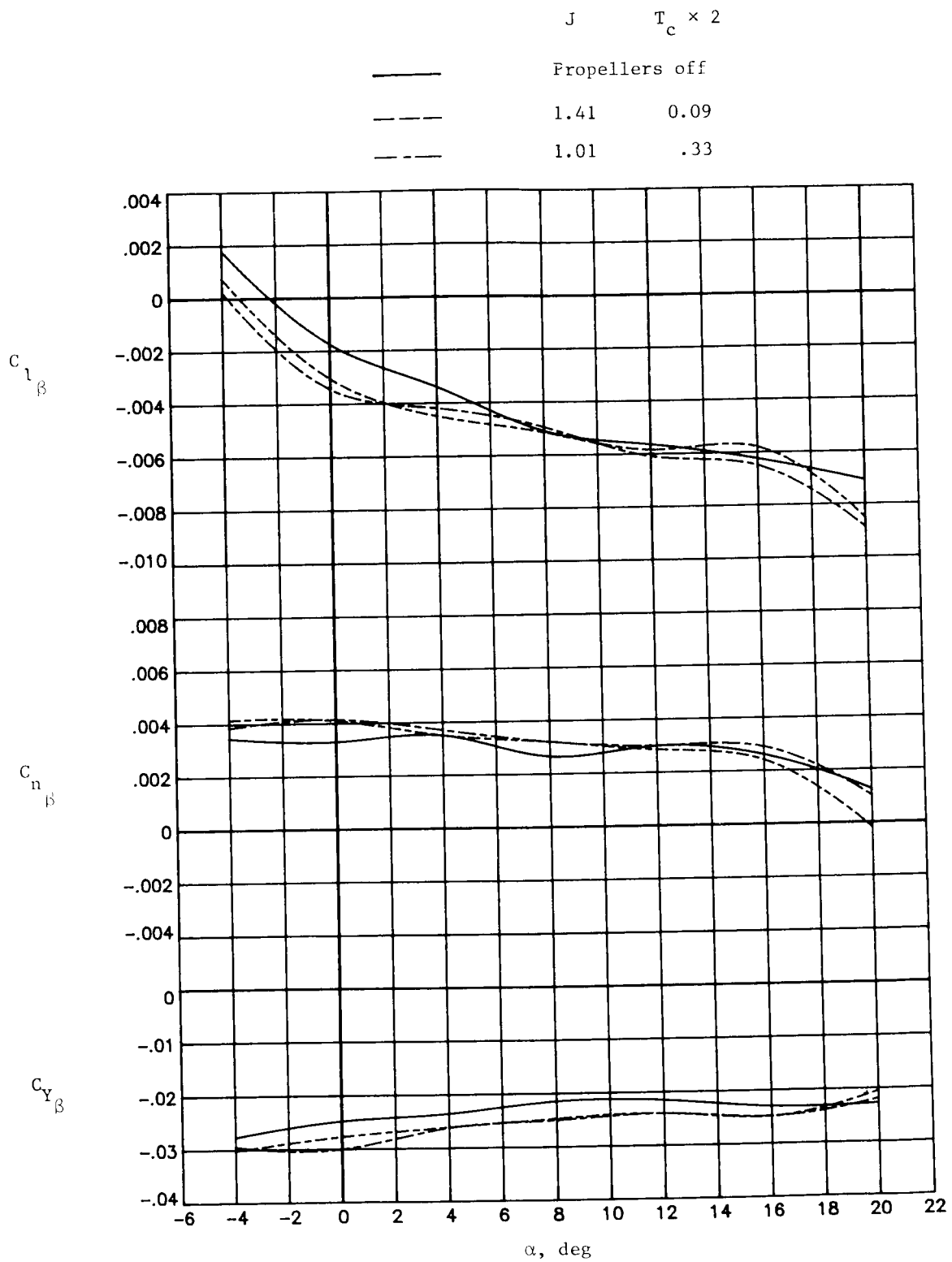
Figure 13. Continued.

	Run	β , deg
○	197	-5
□	191	0
◇	200	5



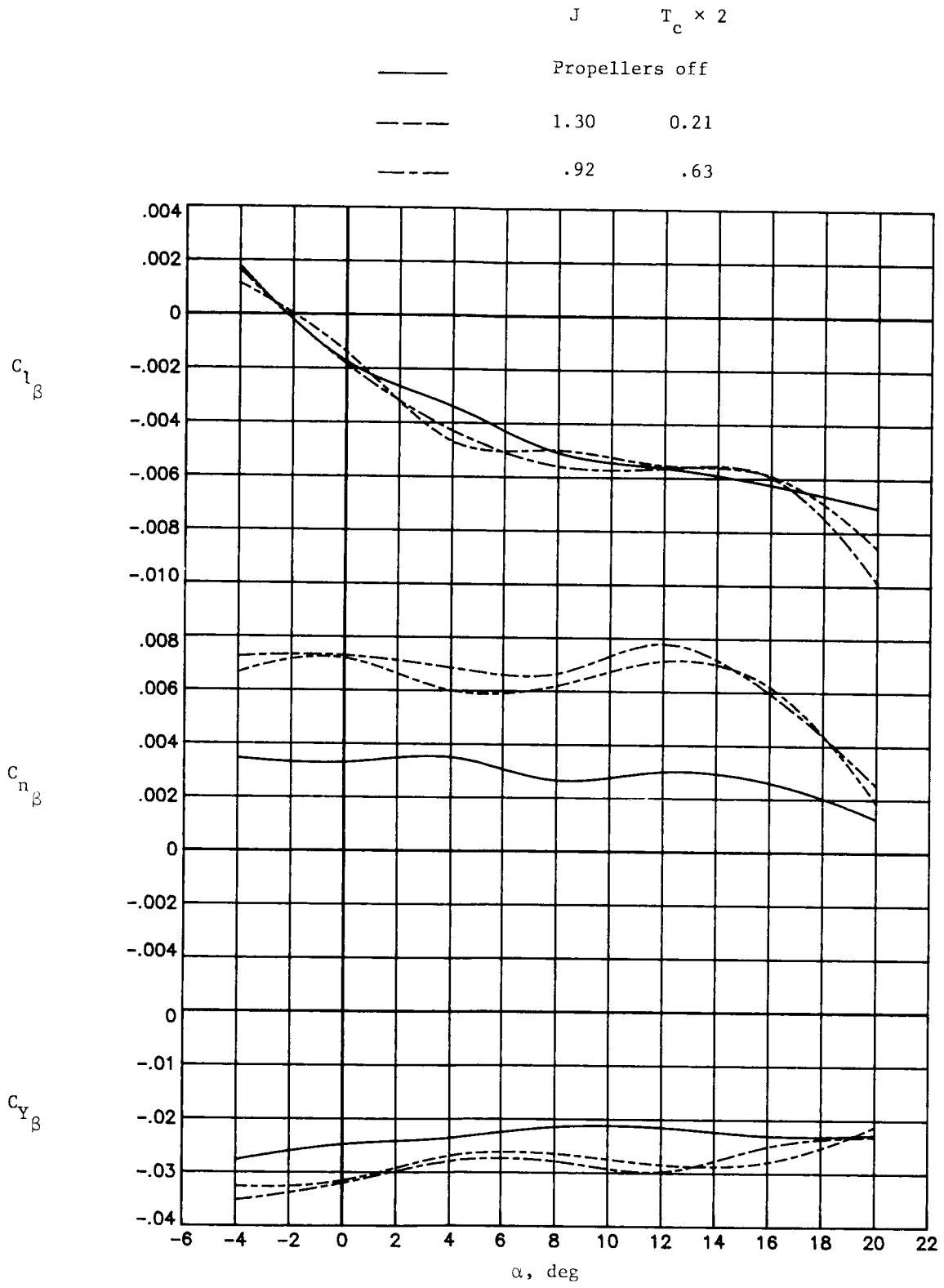
(e) Counter-rotation pusher configuration. $J = 0.92$.

Figure 13. Concluded.



(a) Single-rotation tractor configuration.

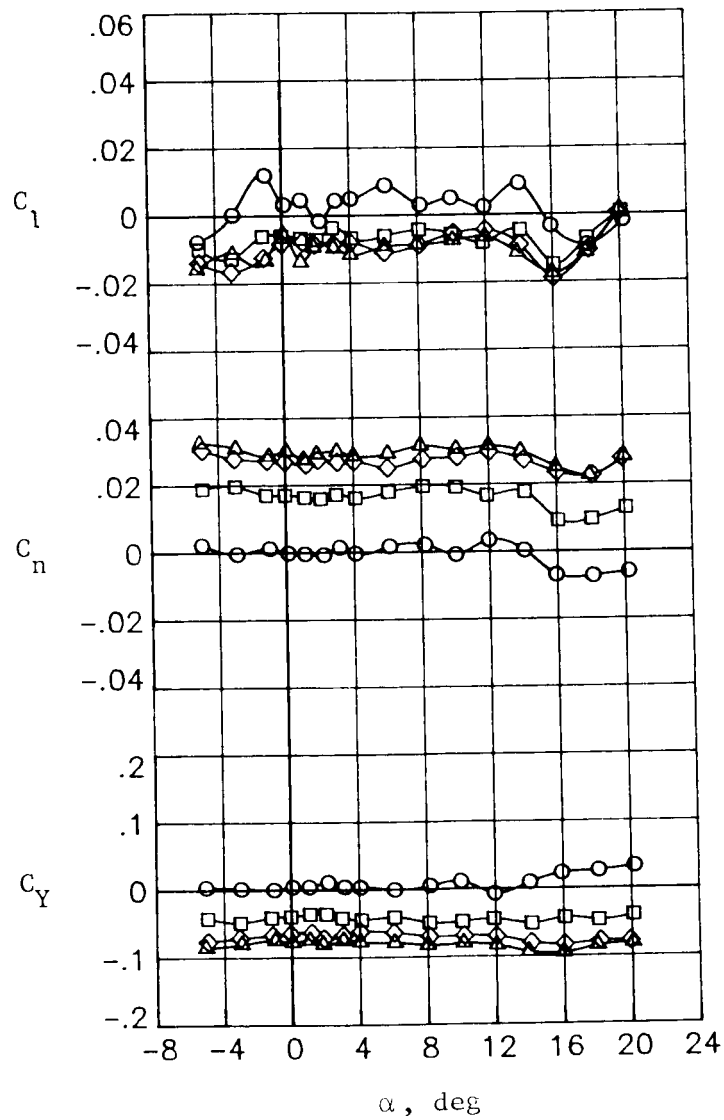
Figure 14. Effect of thrust on static lateral-directional stability derivatives.



(b) Counter-rotation pusher configuration.

Figure 14. Concluded.

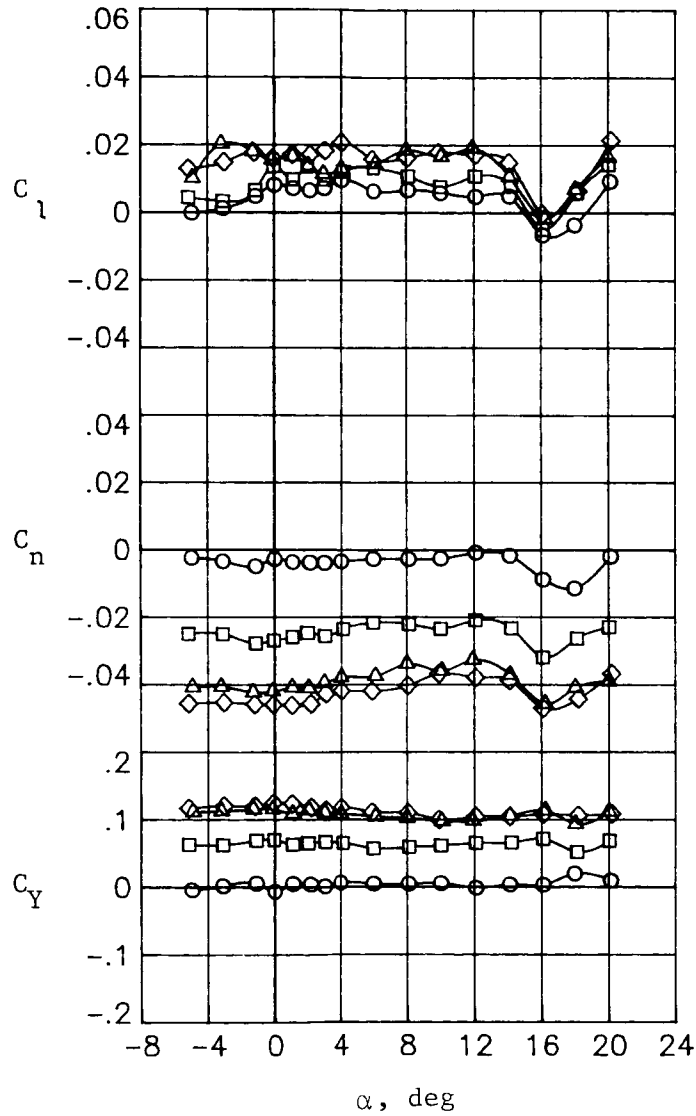
	Run	δ_r , deg
○	374	0
□	279	-10
◇	278	-20
△	277	-30



(a) Power off (propellers off).

Figure 15. Effect of rudder deflection on lateral-directional aerodynamic characteristics.

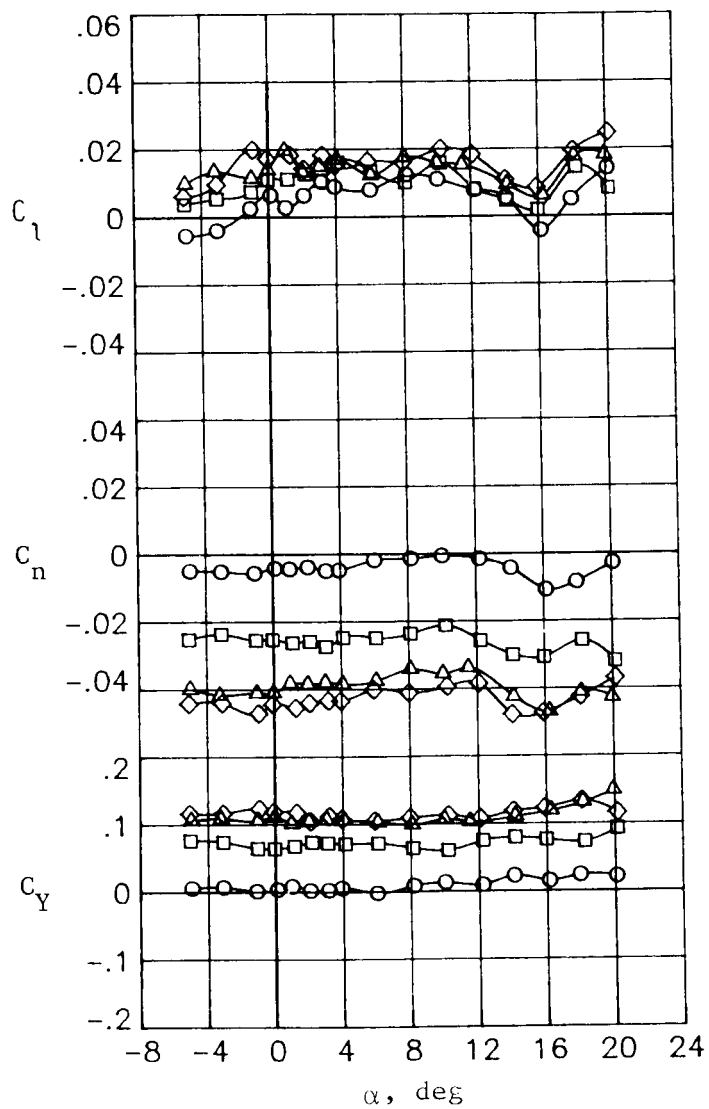
	Run	δ_r , deg
○	299	0
□	332	10
◇	329	20
△	326	30



(b) Single-rotation tractor configuration. $J = 1.41$.

Figure 15. Continued.

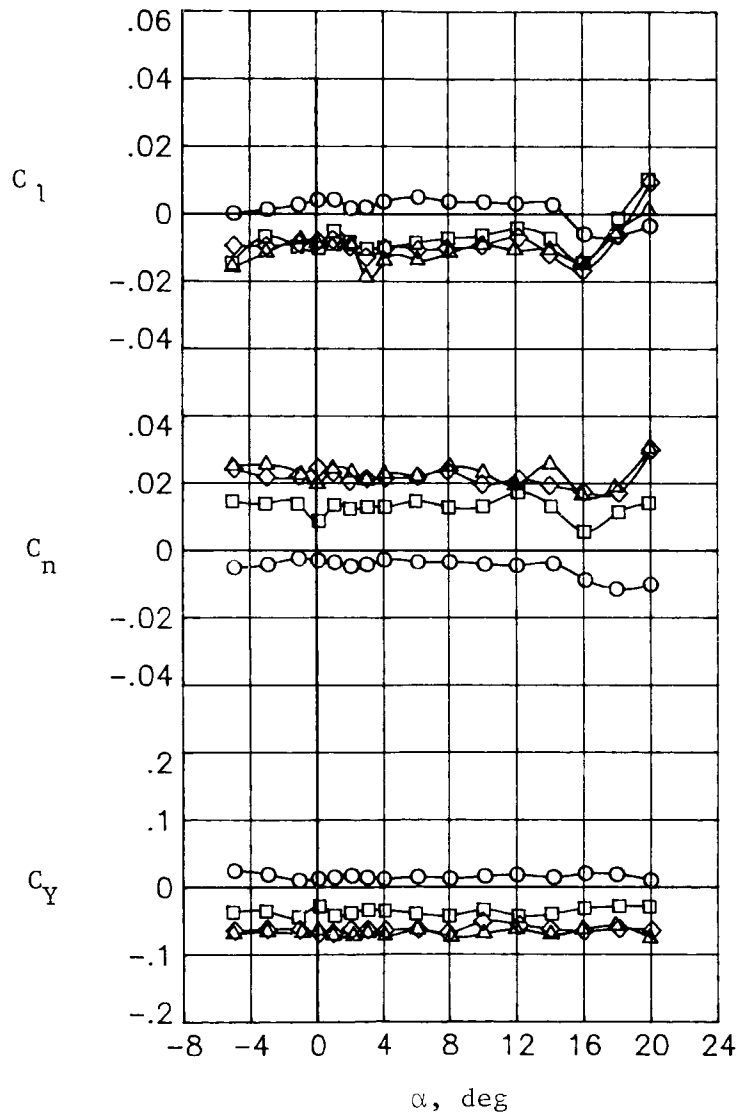
	Run	δ_r , deg
○	298	0
□	331	10
◇	328	20
△	325	30



(c) Single-rotation tractor configuration. $J = 1.01$.

Figure 15. Continued.

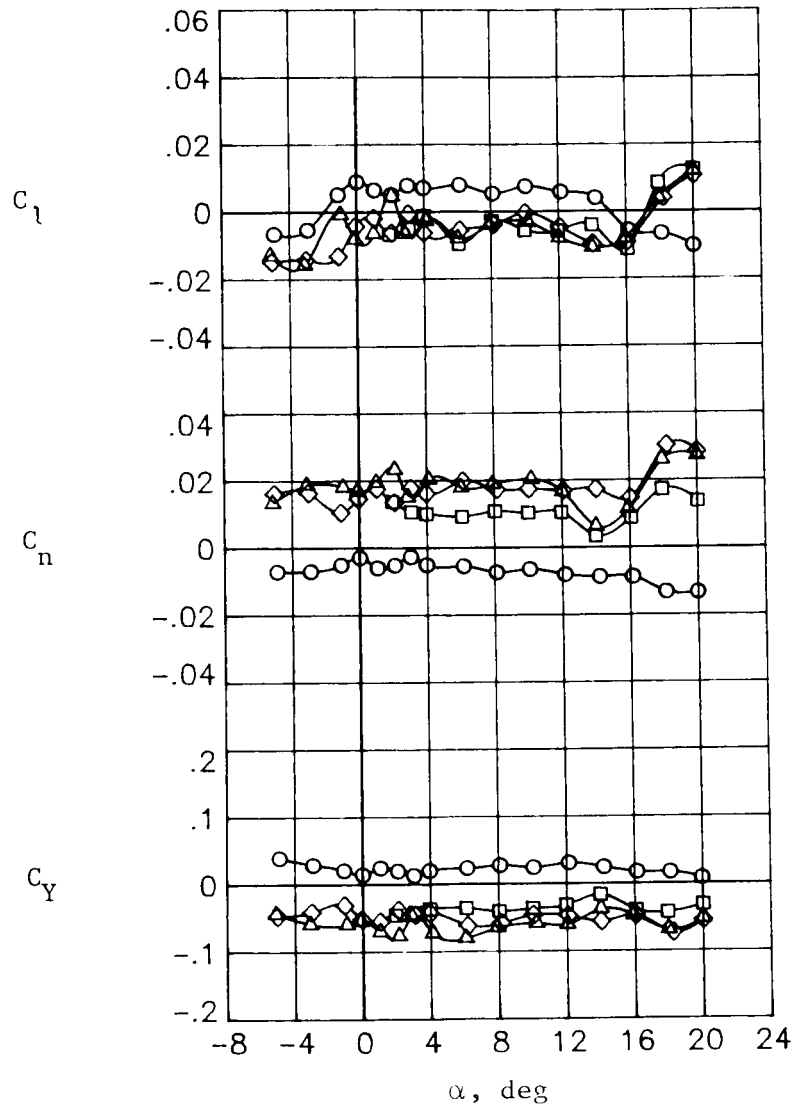
	Run	δ_r , deg
○	192	0
□	231	-10
◇	234	-20
△	237	-30



(d) Counter-rotation pusher configuration. $J = 1.30$.

Figure 15. Continued.

	Run	δ_r , deg
○	191	0
□	230	-10
◇	233	-20
△	236	-30



(e) Counter-rotation pusher configuration. $J = 0.92$.

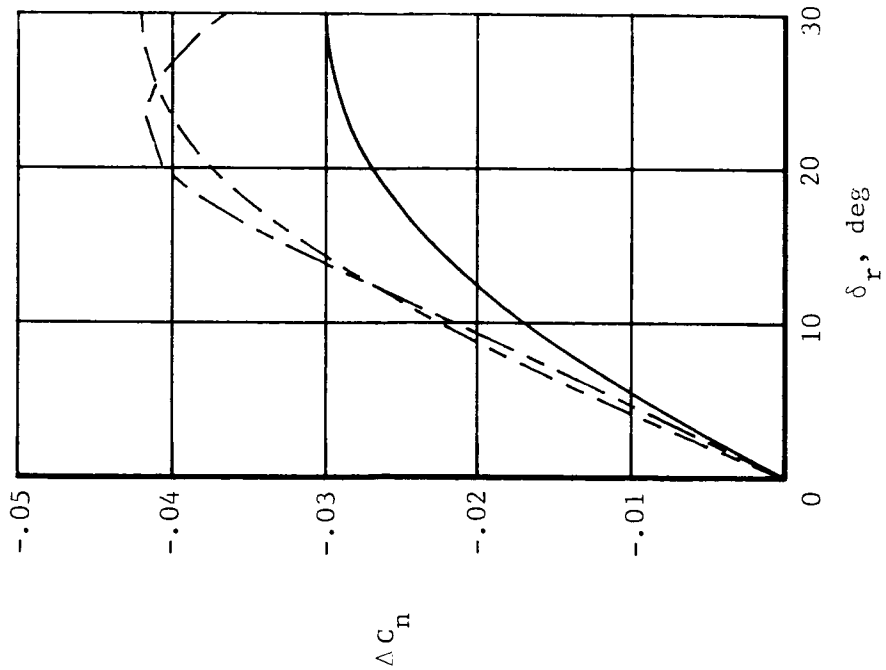
Figure 15. Concluded.

J $T_c \times 2$

Propellers off

1.41 0.09

1.01 .33



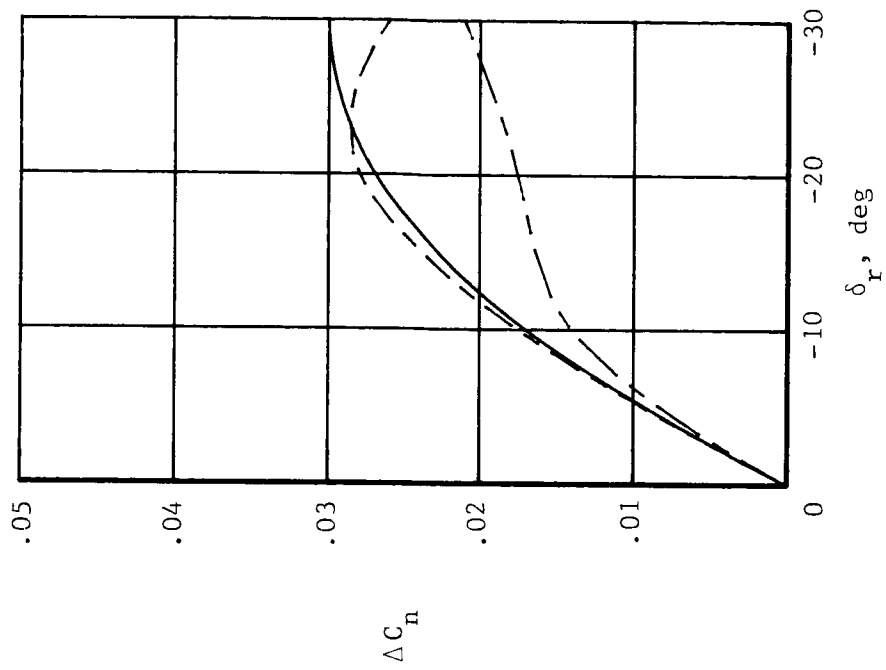
(a) Single-rotation tractor configuration.

J $T_c \times 2$

Propellers off

1.30 0.21

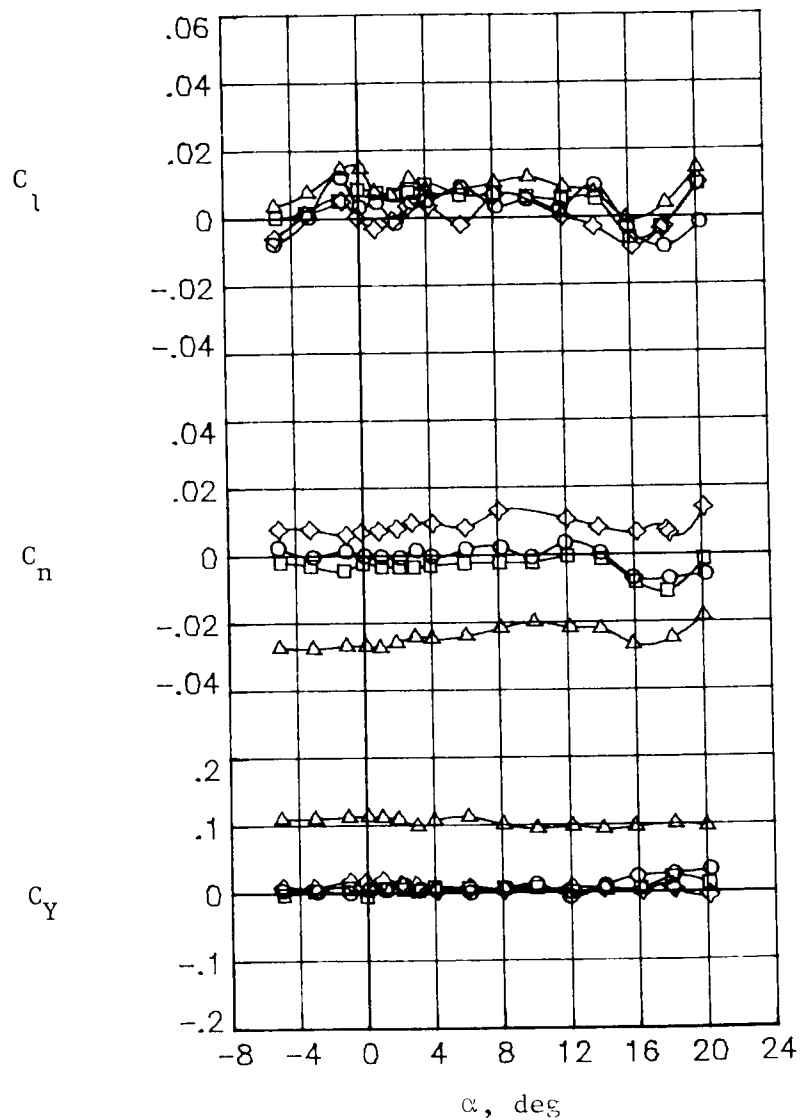
.92 .63



(b) Counter-rotation pusher configuration.

Figure 16. Effect of thrust on rudder control effectiveness. $\alpha = 0^\circ$.

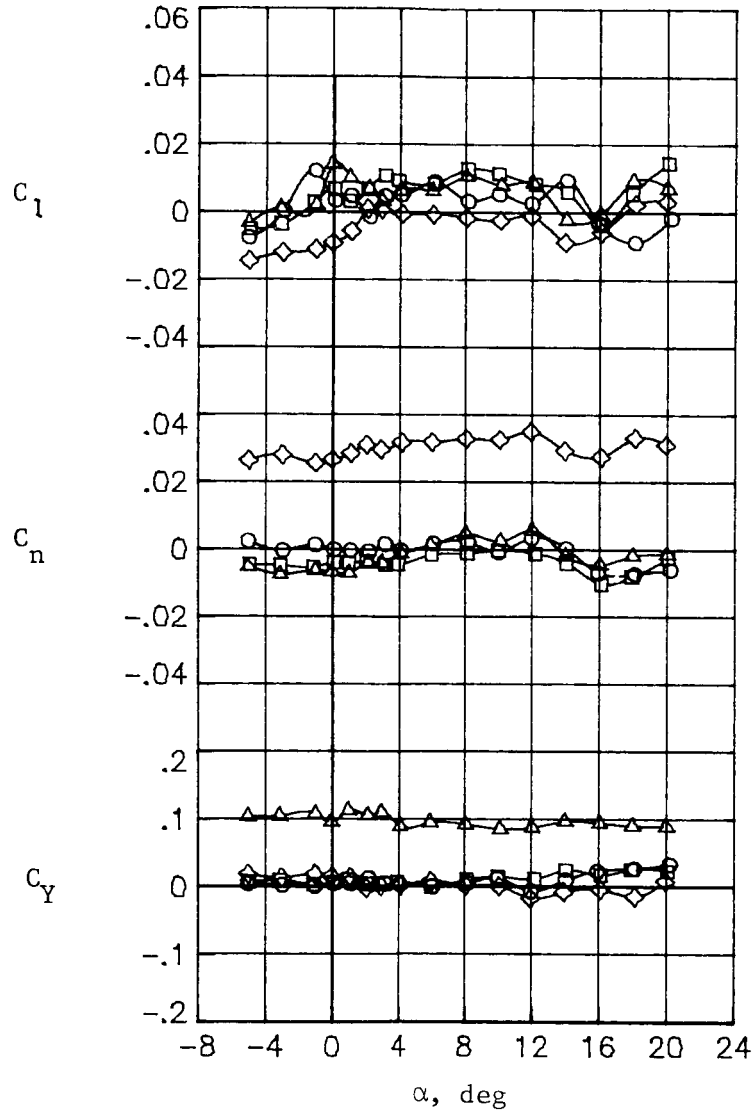
	Run	Power	δ_r , deg
○	374	Propellers off	0
□	299	Symmetric	0
◇	342	Right engine out	0
△	345	Right engine out	30



(a) Single-rotation tractor configuration. $J = 1.41$.

Figure 17. Effect of engine out (propeller windmilling) and rudder deflection on lateral-directional aerodynamic characteristics.

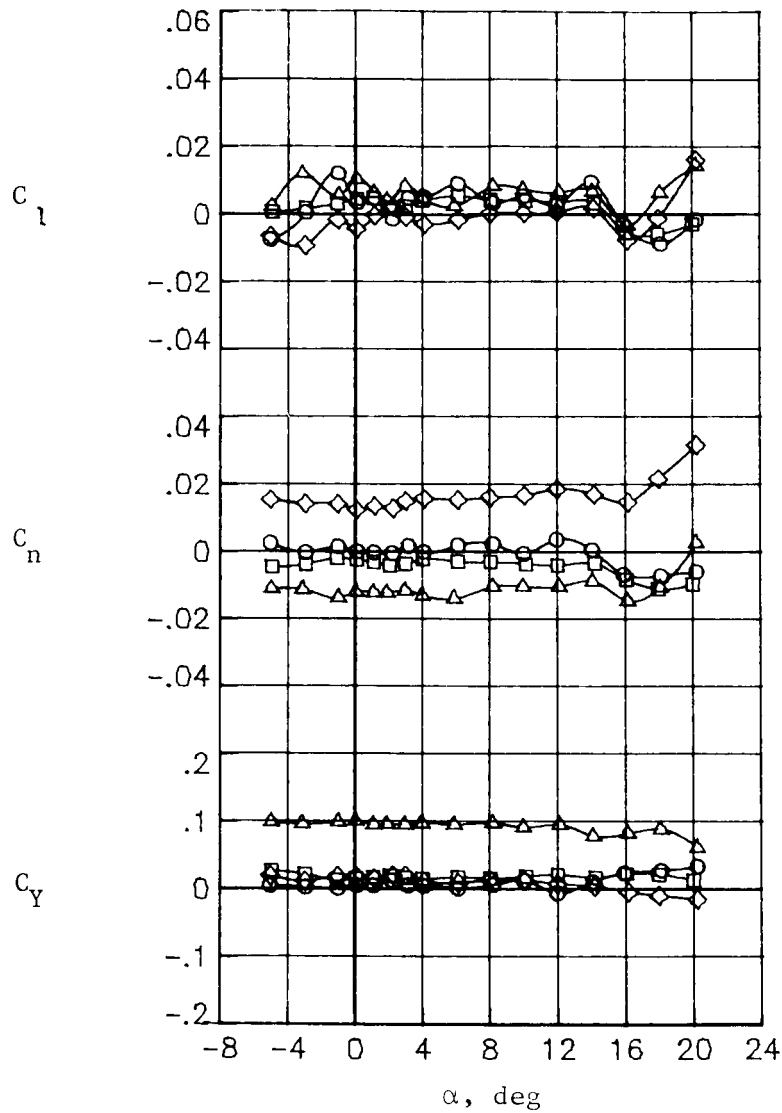
	Run	Power	δ_r , deg
○	374	Propellers off	0
□	298	Symmetric	0
◇	341	Right engine out	0
△	344	Right engine out	30



(b) Single-rotation tractor configuration. $J = 1.01$.

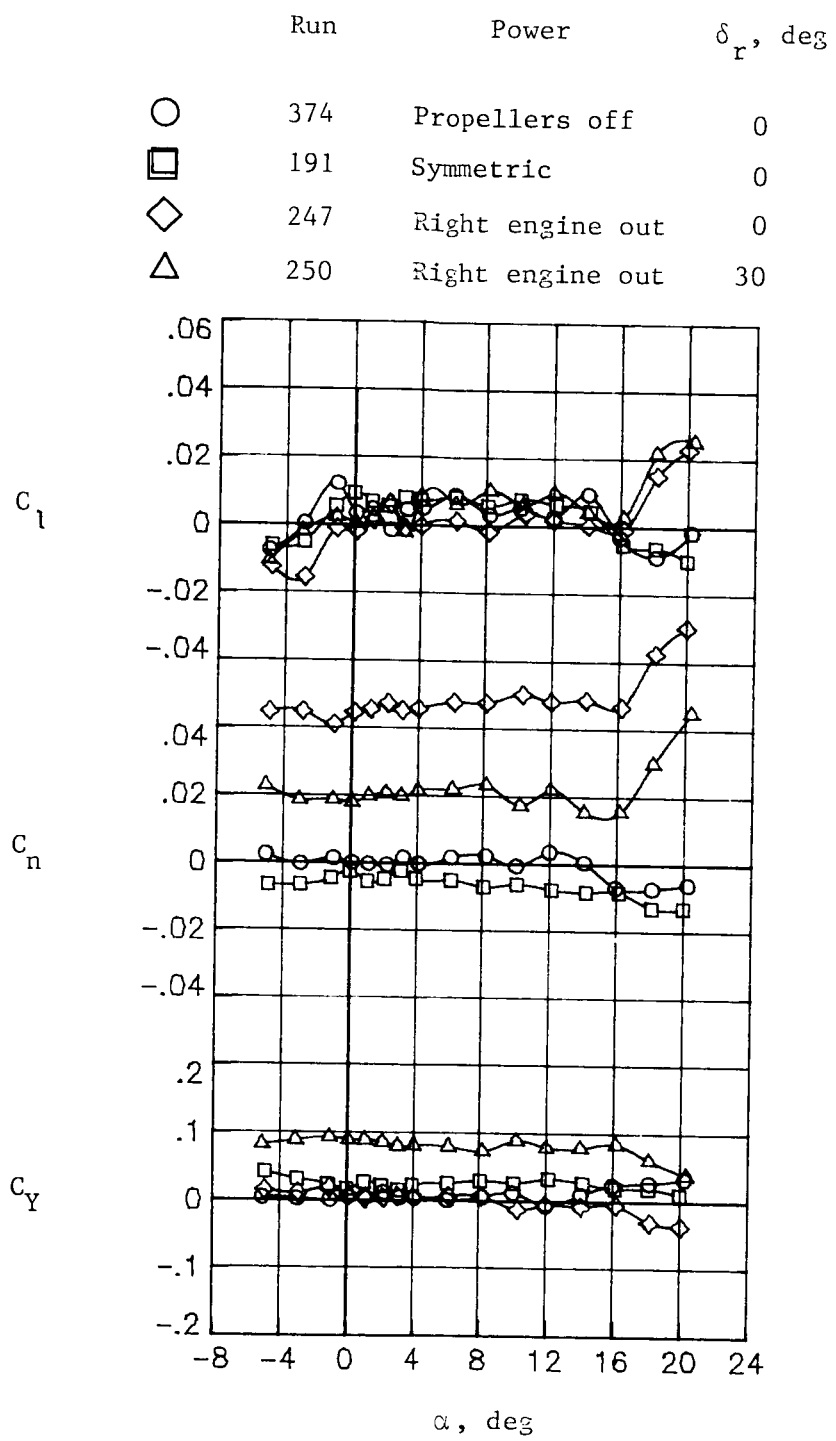
Figure 17. Continued.

	Run	Power	δ_r , deg
○	374	Propellers off	0
□	192	Symmetric	0
◇	248	Right engine out	0
△	251	Right engine out	30



(c) Counter-rotation pusher configuration. $J = 1.30$.

Figure 17. Continued.



(d) Counter-rotation pusher configuration. $J = 0.92$.

Figure 17. Concluded.

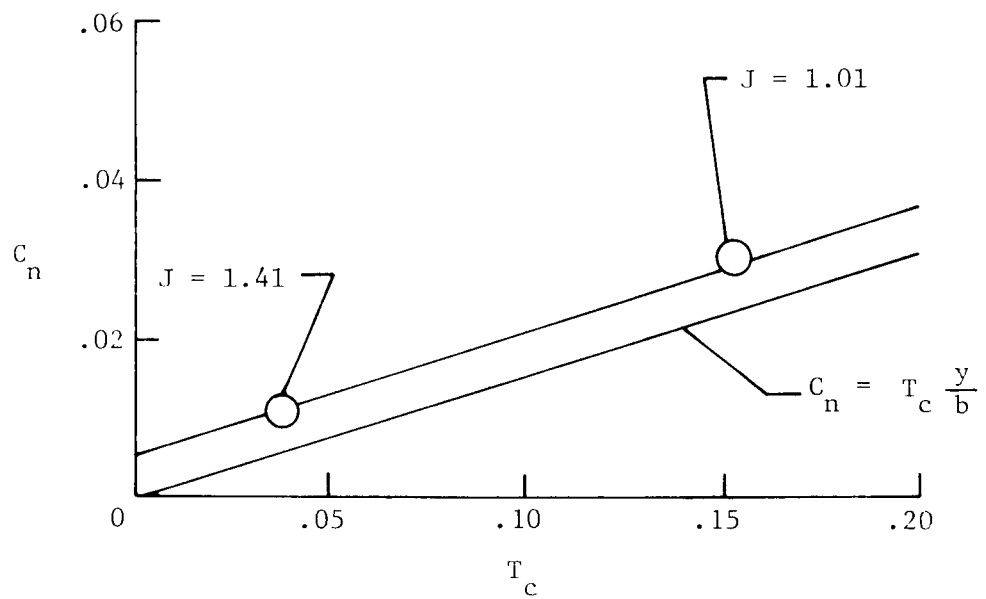


Figure 18. Engine-out yawing moment plotted against thrust for configuration with single-rotation tractor propeller.

References

1. Whitlow, J. B., Jr.: and Sievers, G. K.: *Fuel Savings Potential of the NASA Advanced Turbo Prop Program*. NASA TM-83736. [1984].
2. Goldsmith, I. M.: *A Study To Define the Research and Technology Requirements for Advanced Turbo/Propfan Transport Aircraft*. NASA CR-166138, 1981.
3. Mikkelsen, Daniel C.; Mitchell, Glenn A.; and Bober, Lawrence J.: *Summary of Recent NASA Propeller Research*. NASA TM-83733, [1984].
4. Morgan, Harry L., Jr.; and Paulson, John W., Jr.: *Low-Speed Aerodynamic Performance of a High-Aspect-Ratio Supercritical-Wing Transport Model Equipped With Full-Span Slat and Part-Span Double-Slotted Flaps*. NASA TP-1580, 1979.
5. Morgan, Harry L., Jr.: *Low-Speed Aerodynamic Performance of an Aspect-Ratio-10 Supercritical-Wing Transport Model Equipped With a Full-Span Slat and Part-Span and Full-Span Double-Slotted Flaps*. NASA TP-1805, 1981.
6. Howard, Jenny M.; and Morgan, Harry L., Jr.: *Pressure Distribution Data From Tests of Aspect-Ratio-10 EET High-Lift Research Model Equipped With Part- and Full-Span Flaps*. NASA TM-80082, 1979.
7. Morgan, Harry L., Jr.: *Model Geometry Description and Pressure Distribution Data From Tests of EET High-Lift Research Model Equipped With Full-Span Slat and Part-Span Flaps*. NASA TM-80048, 1979.
8. Block, P. J. W.: *Installation Noise Measurements of Model SR and CR Propellers*. NASA TM-85790, 1984.
9. Coe, Paul L., Jr.; Gentry, Garl L., Jr.; and Dunham, Dana Morris: *Low-Speed Wind-Tunnel Tests of an Advanced Eight-Bladed Propeller*. NASA TM-86364, 1985.
10. Applin, Zachary T.: *Flow Improvements in the Circuit of the Langley 4- by 7-Meter Tunnel*. NASA TM-85662, 1983.
11. Turner, Thomas R.: *Endless-Belt Technique for Ground Simulation. Conference on V/STOL and STOL Aircraft*. NASA SP-116, 1966, pp. 435-446.
12. Gillis, Clarence L.; Polhamus, Edward C.; and Gray, Joseph L., Jr.: *Charts for Determining Jet-Boundary Corrections for Complete Models in 7- by 10-Foot Closed Rectangular Wind Tunnels*. NACA WR L-123, 1945. (Formerly NACA ARR L5G31.)
13. Herriot, John G.: *Blockage Corrections for Three-Dimensional-Flow Closed-Throat Wind Tunnels, With Consideration of the Effect of Compressibility*. NACA Rep. 995, 1950. (Supersedes NACA RM A7B28.)

1. Report No. NASA TP-2535	2. Government Accession No.	3. Recipient's Catalog No.	
4. Title and Subtitle Low-Speed Stability and Control Characteristics of a Transport Model With Aft-Fuselage-Mounted Advanced Turboprops		5. Report Date April 1986	
		6. Performing Organization Code 535-03-12-07	
7. Author(s) Zachary T. Applin and Paul L. Coe, Jr.		8. Performing Organization Report No. L-16004	
		9. Performing Organization Name and Address NASA Langley Research Center Hampton, VA 23665-5225	
12. Sponsoring Agency Name and Address National Aeronautics and Space Administration Washington, DC 20546-0001		10. Work Unit No.	
		11. Contract or Grant No.	
15. Supplementary Notes		13. Type of Report and Period Covered Technical Paper	
		14. Sponsoring Agency Code	
16. Abstract A limited experimental investigation was conducted in the Langley 4- by 7-Meter Tunnel to explore the effects of aft-fuselage-mounted advanced turboprop installations on the low-speed stability and control characteristics of a representative transport aircraft in a landing configuration. In general, the experimental results indicate that the longitudinal and lateral-directional stability characteristics for the aft-fuselage-mounted single-rotation tractor and counter-rotation pusher propeller configurations tested during this investigation are acceptable aerodynamically. For the single-rotation tractor configuration, the propeller-induced aerodynamics are significantly influenced by the interaction of the propeller slipstream with the pylon and nacelle. The stability characteristics for the counter-rotation pusher configuration are strongly influenced by propeller normal forces. The longitudinal and directional control effectiveness, engine-out characteristics, and ground effects are also presented. In addition, a tabulated presentation of all aerodynamic data presented in this report is included as an appendix.			
17. Key Words (Suggested by Authors(s)) Advanced turboprops Counter-rotation propeller Stability and control Aerodynamic characteristics		18. Distribution Statement Unclassified—Unlimited Subject Category 08	
19. Security Classif.(of this report) Unclassified	20. Security Classif.(of this page) Unclassified	21. No. of Pages 66	22. Price A04

**National Aeronautics and
Space Administration
Code NIT-4**

**Washington, D.C.
20546-0001**

**Official Business
Penalty for Private Use, \$300**

**BULK RATE
POSTAGE & FEES PAID
NASA
Permit No. G-27**

NASA

**POSTMASTER: If Undeliverable (Section 158
Postal Manual) Do Not Return**
